UPPSALA UNIVERSITET

UPTEC X 26022
Examensarbete 30 hp
June 2026

# Enhancing Sensitivity of Alzheimer's Biomarker Detection Using BOLD (Binding Oligo Ladder Detection)

## Development and Optimization of the BOLD-amplified Standard ELISA Assay

Annie Sernelin

Civilingenjörsprogrammet i molekylär bioteknik

UPPSALA UNIVERSITET

# Enhancing Sensitivity of Alzheimer's Biomarker Detection Using BOLD (Binding Oligo Ladder Detection)

Annie Sernelin

## Abstract

ELISA (Enzyme-Linked Immunosorbent Assay) is an analytical tool frequently used for the detection and quantification of biomolecules. It is frequently used within diagnostics for measurement of biomarkers such as hormones, antibodies or proteins related to different diseases. Levels of biomarkers often vary in healthy and diseased patients; it can therefore be a very helpful approach for assessing patient status. Amyloid beta (Aβ) proteins are one of the most prominent biomarkers associated with Alzheimer's disease. They stem from incorrect cleavage of the amyloid precursor protein (APP) creating toxic peptides with high tendencies to aggregate and form large, insoluable structures called plaques. Measurement of Aβ is often done in cerebrospinal fluid (CSF) or through positron emission tomography (PET), methods that poses many challenges. As an alternative, researchers have begun investigating possible measurements of Aβ in blood, often requiring special signal amplification techniques due to low concentration levels.

This project aimed to develop and optimize a signal amplified sandwich ELISA assay that can detect and quantify Aβ in blood. The center of this assay is the add-on reagent Exazym® containing Cavidi's Binding Oligo Ladder Detection (BOLD) technology that uses primer-conjugated secondary antibodies, DNA-synthesis and DNA-specific tertiary antibodies to amplify the signal and increase the sensitivity of the assay. By optimizing assay components and protocol parameters such as incubation time, blocking buffers and antibody concentrations, the background noise was reduced from 0.6 OD to 0.1 OD. Furthermore, in comparison to the standard ELISA assay, increase of signals with BOLD-amplification ranged from 2-fold to 10-fold with increasing Aβ concentration. Lastly, the initial estimation of assay performance illustrated great potential regarding assay sensitivity with an LLOQ of 1.42 pg/mL, a value in the range of similar products available on the market.

**Teknisk-naturvetenskapliga fakulteten**

**Uppsala universitet, Utgivningsort Uppsala**

Handledare: Peter Stenlund Ämnesgranskare: Ylva Ivarsson

Examinator: Johan Åqvist

# Implementering av BOLD-teknik för förbättrad biomarkördetektion vid Alzheimers sjukdom

## Populärvetenskaplig sammanfattning

**Annie Sernelin**

Alzheimers sjukdom, den vanligaste formen av demens, påverkar tiotals miljoner äldre varje år. Sjukdomen är neurodegenerativ och orsakar nedbrytning av celler i nervssystemet, såsom i hjärnan, vilket gradvis leder till nedsatta kognitiva funktioner och beteendeförändringar. Nedbrytningen associeras till specifika proteiner bl.a amyloid-beta (Aβ) proteiner och hyperfosforylerat tau (pTau) som klumpar ihop sig och stör basala funktioner såsom signalöverföring i hjärnan. ELISA är en metod som använder enzymer och antikroppar för att mäta hur mycket av dessa proteiner som finns i ett prov. Aβ-proteiner mäts ofta i ryggmärgsvätska men då det är en ganska invasiv provtagning vill man undersöka möjligheten att kunna mäta samma sak i blod. Problemet är att det finns mycket längre halt av Aβ i blodet och ELISA kan bara mäta ned till en viss koncentration. För att göra detta möjligt är det många som forskar på metoder som kan förstärka signalen.

Cavidi AB är ett företag som har utvecklat Exazym®, ett reagens-kit som är baserad på en metod som kallas BOLD, Binding Oligo Ladder Detection. BOLD utnyttjar DNA-molekyler för att kunna binda fler signalmolekyler till det uppfångade proteinet. Signalen blir då starkare jämfört med standardmetoden som använder endast en signalmolekyl. Följande projekt syftade till att utveckla och optimera en högkänslig detektionsmetod för Alzheimers biomarkörer genom att integrera BOLD-tekniken i ett standard ELISA format. Först genomfördes konjugering av detektorantikropparna med olika ratio av primer följt av testning tillsammans med olika uppfångningsantikroppar. Den mest lovande kombinationen var RmAb158 antikroppen för uppfångning och en primerkonjugerad 3D6 antikropp för detektion då detta gav lägst bakgrundsbrus i absorbansmätningarna. Vidare undersöktes olika strukturella former av antigen, monomerer och protofibriller, där en uppenbart starkare signal sågs med protofibrillerna. Optimering av standardprotokollet krävdes för att minska det initiala bakgrundsbruset. Många olika parametrar testades, bla inkuberingstid av antikroppar och antigen, diluenter och blocknings buffrar samt olika antikroppskoncentrationer. Det slutliga protkollet med kortare inkubationstider och sänkt detektorantikroppskoncentration visar tydligt att med BOLD fås mellan 2-10 gånger högre signaler jämfört med standardmetoden. Den initiala uppskattningen av precisionen på assayn visar också mycket lovande värden i känslighet, jämförbart med assays på marknaden.

# Table of contents

**Abbreviations** ..... 10

**1 Introduction** ..... 1
1.1 Aim and Objectives ..... 3

**2 Background** ..... 3
2.1 Amyloid Beta and Alzheimer's Disease ..... 3
2.2 Antibodies ..... 7
2.3 ELISA and Immunoassays ..... 9
2.4 Signal Amplification with BOLD ..... 11
2.5 Precision and Reliability in Assay Development ..... 12

**3 Materials and Methods** ..... 14
3.1 Materials ..... 14
3.1.1 Antibodies ..... 14
3.1.2 Antigen ..... 14
3.1.3 Reagents ..... 14
3.2 Methods ..... 15
3.2.1 Reverse ClickChem Conjugation of Detector Antibody ..... 15
3.2.2 Micro BCA Assay ..... 15
3.2.3 SDS PAGE ..... 16
3.2.4 Biotinylation of Detector Antibodies for the Standard ELISA ..... 16
3.2.5 Direct ELISA for Confirmation of Successful Biotinylation ..... 16
3.2.6 Capture and Detector Antibodies ..... 17
3.2.7 Standard ELISA Protocol ..... 17
3.2.8 BOLD-amplified Standard ELISA Protocol ..... 18
3.2.9 Optimized Final BOLD-amplified Standard ELISA Protocol ..... 18
3.2.10 Statistics and Analysis of Absorbance Data ..... 19

**4 Results** ..... 20

4.1 Validation and Quantification of Reverse-conjugated Oligo-dT Detector Antibodies and Biotinylated Detector Antibodies ..... 20
4.2 Evaluation of Antigen, Capture and Detector Antibody ..... 21
4.3 Evaluation of Background Noise Reduction Strategies in the BOLD-amplified ELISA ..... 23
4.3.1 Incubation Time ..... 24
4.3.2 Blocking Buffers and Diluents ..... 28
4.3.3 Detector Antibody Concentrations ..... 30
4.3.4 Initial Estimation of Assay Precision ..... 32

**5 Discussion** ..... 36
5.1 Evaluation of Antibodies and Antigen for the BOLD-amplified Assay 36
5.2 Shortened Incubation Time for Reduced Background Noise ..... 38
5.3 Successful Combination of Blocking Agents ..... 39
5.4 Incresed SNR with Higher Detector Antibody Concentration ..... 40
5.5 Initial Estimation of Assay Precision ..... 41
5.6 Relevance ..... 42

**6 Future research** ..... 42

**7 Conclusion** ..... 43

**Ethical Considerations** ..... 44

**AI Statement** ..... 45

**Acknowledgements** ..... 45

**References** ..... 46

**A Supplementary Tables** ..... 53
A.0.1 Conjugation of Antibodies ..... 53

A.0.2 Biotinylation of Antibodies ..... 54
A.0.3 Initial Estimation of Assay Precision ..... 55

**B Supplementary Figures** ..... 56

**C Supplementary Methods** ..... 59

**D Code Details** ..... 62
D.1 Code Used in the BCA Analysis: ..... 62
D.2 Code Used in the ELISA Precision Analysis : ..... 64

# Abbreviations

| | |
|---|---|
| $A\beta 40$ | Amyloid beta 40 |
| $A\beta 42$ | Amyloid beta 42 |
| $A\beta$ | Amyloid beta |
| $AA$ | Amino acid |
| $Ab$ | Antibody |
| $Ag$ | Antigen |
| $BCA$ | Bicinchoninic acid |
| $Blck$ | Blocking buffer |
| $BOLD$ | Binding Oligo Ladder Detection |
| $BrdUTP$ | 5-bromo-2′-deoxyuridine-5′-triphosphate |
| $BSA$ | Bovine Albumin Serum |
| $Capt$ | Capture |
| $cDNA$ | Complementary DNA |
| $CSF$ | Cerebrospinal fluid |
| $DBCO$ | Dibenzocyclooctyne |
| $Det$ | Detector |
| $dH2O$ | Deionized water |
| $DMSO$ | Dimethylsulfoxide |
| $DTT$ | Dithiothreitol |
| $ELISA$ | Enzyme-Linked Immunosorbent Assay |
| $kDa$ | kiloDalton |
| $LB$ | Low Bind |
| $mAb$ | Monoclonal antibody |

| | |
|---|---|
| $MW$ | Molecular Weight |
| $NFTs$ | Neurofibrillary Tangles |
| $oligo - dT$ | Oligo deoxithymidine |
| $PBS$ | Phosphate Buffered Saline |
| $PBST$ | PBS + 0.05% Tween 20 |
| $PET$ | Positron Emission Tomography |
| $prA$ | Poly-adenine ribose |
| $pTau$ | Phosphorylated Tau |
| $RT$ | Room Temperature |
| $SA - HRP$ | Streptavadin horseradish peroxidase |
| $SDS\ PAGE$ | Sodium Dodecyl Sulfate–Polyacrylamide Gel Electrophoresis |
| $Std$ | Standard |
| $TEG$ | Triethylene Glycol |
| $TMB$ | 3,3′,5,5′-Tetramethylbenzidine |
| $Vol$ | Volume |
| $WHO$ | World Health Organization |

# 1 Introduction

Dementia affects millions of people around the world. In 2021, WHO estimated the number to be around 57 million people. By 2050, this number is expected to increase to 132 million, raising the demand for preventiton and treatment, and further straining the available resources. In addition to the rising numbers, there is a large portion of undetected cases of dementia (WHO 2017). In an article from Lang et al (2017) that analyzed 23 international studies, the estimated number of undiagnosed dementia cases is more than 60% (Lang *et al.* 2017).

About 70 % of the dementia cases are attributed to Alzheimer's disease (AD), the most common form of dementia (WHO 2025). AD is an irreversible, neurogenerative condition that progressively leads to impairment of cognitive and behavioural functions such as memory, comprehension, language, attention and reasoning (Kumar *et al.* 2025). Its pathogenesis has been attributed to the formation of amyloid β (Aβ) plaques and neurofibrillary tangles (NFTs) that disrupt communication between neurons and affect signal processing, ultimately leading to neuronal death (Tiwari *et al.* 2019).

AD is primarily discovered in the elderly, ages 65 and up, with increasing numbers in younger people from the age of 40 (Zeliger 2023). The majority of current AD treatments are focused on symptom management and the few that have disease-modifying effects aim to reduce the toxic forms of protein aggregates (Kumar *et al.* 2025). Lecanemab and Donanemab are two such pharmaceuticals that use anti-amyloid antibodies to clear Aβ proteins from the brain and thus preventing further aggregation into plaques (Elamin *et al.* 2025). Although they claim to have disease-modifying effects, it is important to point out that these types pharmaceuticals are only able to slow cognitive decline, not halt disease progression. It has also been proven that the best effect is seen on patients in the early stages of AD (Dyck *et al.* 2023).

AD neuropathology can begin up to 20 years before any symptoms are exhibited. (Alawode *et al.* 2022). Tailoring treatment for those affected by the disease thus requires information about the underlying pathological processes and the stage of progression, especially since many of the available amyloid-clearing pharmaceuticals require an early stage diagnosis (del Campo *et al.* 2015). Assessing patient status can be done though detection and analysis of biomarkers (Gunes *et al.* 2022). Biomarkers are biomolecules whose levels differ between healthy individuals and those affected by disease (Arya & Estrela 2018). The measurement of certain biomarkers such as Aβ or pTau can therefore be used as an aid in setting an AD diagnosis.

There are two frequently used methods for detecting AD biomarkers: Analysis of the

Cerebrospinal fluid (CSF) and Positron Emission Tomography (PET) (Schöll *et al.* 2024). CSF collection, or lumbar puncture, is done by inserting a needle in the spine and collecting fluid (Margetis & Baker 2025), the CSF is then analyzed using automated immunoassays (Bouwman *et al.* 2022). Lumbar puncture is often considered to be a very invasive procedure and it places a high physical burden on the patient (Gunes *et al.* 2022). PET scans on the other hand, involve injecting brain-tissue-absorbing radiotracers. By collecting the gamma rays emitted by the tracers, the activity can be assessed and the distribution of biomarkers in the tissues can be converted into a 3D image. (Kapoor *et al.* 2025). While PET is less invasive and considered to be more informative (Zarovniaeva *et al.* 2025), it often requires very expensive infrastructure (Gunes *et al.* 2022). For these reasons, there is a need for finding alternative methods sensitive enough to detect an early progression, not only at a clinical level but also at a primary care level where the disease is often initially diagnosed (Porsteinsson *et al.* 2021).

An alternative sample type with great potential that addresses the issues associated with CSF and PET, is blood biomarkers. Blood biomarkers are the same fluid biomarkers found in CSF but with a less invasive sample collection (Schöll *et al.* 2024). One common method for measurement of different blood biomarkers is enzyme-linked immunosorbent assay (ELISA) (Hu *et al.* 2020). ELISA generally utilizes the catalytic effect of enzymes to detect and quantify immunologic reactions. The four major types of ELISA are direct ELISA, indirect ELISA, sandwich ELISA and competitive ELISA. Depending on the type of ELISA, the testing often require slightly different components and steps, sandwich ELISA for example uses two antibodies with different epitopes, one capture antibody and one biotinylated antibody for capture (Alhajj *et al.* 2025). This is considered to be the most sensitive method, being 2-5 times more sensitive than the other ELISA methods (Aydin *et al.* 2025).

Although the biomarkers in the blood and CSF are the same, recent research reports that there are several clearance mechanisms of Aβ peptides from the brain, leading to 100-fold lower concentrations in blood. To measure these low protein levels in plasma, a highly sensitive assay is required (Mehta *et al.* 2020). ELISA tests are generally known to be robust and well established but they have limited detection sensitivity ($\geq$ 1 pM) which might be insufficient for the detection of small amounts of biomarkers in the early stages of Alzheimer's. (Hu *et al.* 2020). To address this issue, many researchers and companies have begun investigating possible signal amplification techniques.

Cavidi AB is a company that provides researchers with signal amplification solutions for immunoassays. The add-on reagent Exazym® is based on a novel method called BOLD (Binding Oligo Ladder Detection) that utilizes DNA synthesis and multiple tertiary antibodies to amplify immunoassay signals, thereby increasing the sensitivity of the system and lowering the limit of detection. This makes it possible to detect low biomarker con-

centrations present in complex biological samples. The flexibility and possibilities for adaptation allow the solution to be applied to several types of immunoassay platforms for a broad range of research applications such as development of pharmaceuticals or improvement of diagnostic tools.

## 1.1 Aim and Objectives

The aim of this study is to develop and optimize an immunoassay for the detection of biomarkers related to Alzheimer's disease. By integrating the BOLD technology into a standard ELISA format, the immunoassay will be developed to detect low levels of biomarkers such as Aβ40, Aβ42, including monomers, aggregates, and protofibrils in complex biological matrices. Its performance will be evaluated and compared to a standard ELISA.

This project aims to give a better understanding of how implementing new techniques can improve the sensitivity of immunoassays. An increased sensitivity will hopefully lower the detection limits for biomarkers associated with Alzheimer's disease. Earlier detection and diagnosis in patients enables the start of treatments before any major neurodegeneration and cognitive decline has begun, hopefully leading to a slowed disease progression.

In the long run, the results are expected to improve biomarker-detection research and be a part in the development of future therapeutics and diagnostics.

# 2 Background

## 2.1 Amyloid Beta and Alzheimer's Disease

Since the first introduction of Alzheimer's disease by Alois Alzheimer in 1907 (MacLeod *et al.* 2015), the formation of aggregated Aβ plaques and NFTs has been revealed to be key pathophysiological mechanisms (Tiwari *et al.* 2019). In the present context, this event is commonly referred to as the amyloid hypothesis. The amyloid hypothesis describes the initial disease-triggering event as the imbalance in Aβ production and clearance that leads to Aβ accumulation in neuronal tissue and ultimately, the formation of NFTs (MacLeod *et al.* 2015).

Aβ is a 39-43 AA protein derived from the amyloid precursor protein (APP). It is generated by several cell types such as neurons, astrocytes and fibroblasts and is believed to have a significant role in cell development and homeostasis (Azargoonjahromi 2024). APP is a single-pass transmembrane protein with large extracellular domains that is produced in large quantities in neurons and is metabolized in many proteolytic pathways such as neuronal development, transport and signaling (Chen *et al.* 2017) (O'Brien & Wong 2011). APP exists in an array of differently spliced isoforms in different lengths, the form most commonly expressed in the central nervous system and neurons being 695 amino acids long (O'Brien & Wong 2011). Of these 695 amino acids, 28 make up Aβ and an additional 14 amino acids make up the transmembrane domain (Tiwari *et al.* 2019).

Although APP is not toxic within itself, when in a diseased state it can generate amyloidogenic fragments through cleavage with the enzymes $\alpha$-secretase, $\beta$-secretase and $\gamma$-secretase (Tiwari *et al.* 2019). $\alpha$-secretase cleaves within the Aβ domain, $\beta$-secretase at the N-terminal of the domain and $\gamma$-secretase at the C-terminal (MacLeod *et al.* 2015). The cleavage can be non-amyloidogenic, in which the cleavage occurs through $\alpha$-secretase and $\gamma$-secretase under regulated conditions creating non-toxic, soluble fragments that are involved in synaptic signaling (Tiwari *et al.* 2019). Since this pathway does not produce complete Aβ, these fragments are not involved in AD (MacLeod *et al.* 2015). Amyloidogenic cleavage is performed by $\beta$-secretase and $\gamma$-secretase which releases different isoforms of insoluble and toxic Aβ peptides (Tiwari *et al.* 2019). The length of these peptide is determined by the $\gamma$-secretase cut on the C-terminal, most commonly resulting in a 40 AA (Aβ40) or 42 AA (Aβ42) peptide (Johansson *et al.* 2024).

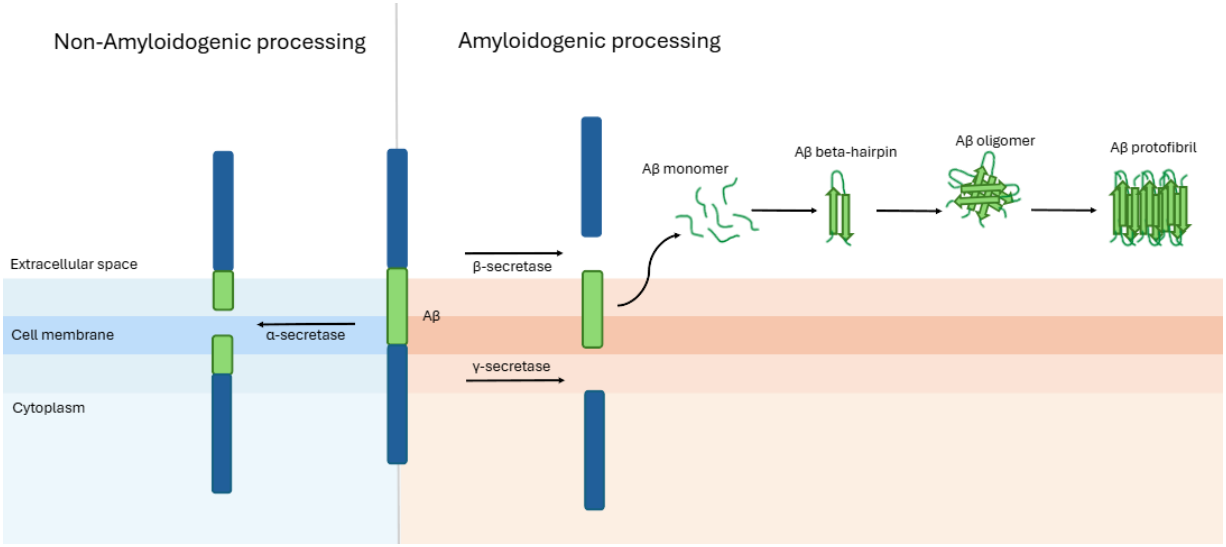


*Figure 1: Illustration of the non-amyloidogenic and amyloidogenic processing of APP including the aggregation stages of amyloid beta. The illustration was created using Microsoft Powerpoint.*

Aβ monomers aggregate into a great weight-range of oligomeric assemblies, such as dimers, trimers and tetramers stretching to protofibrils and fibrils (Chen *et al.* 2017). The aggregation has reported to begin with the formation of an Aβ hairpin triggering the misfolding of additional monomers and later the formation of oligomers. It is also believed that the hairpins go through a conformational change, forming parallel beta sheets (Metzendorf *et al.* 2025). Smaller oligomeric structures are often soluble with a high beta-sheet content, while fibrils are generally insoluble due to the significant aggregation (Chen *et al.* 2017). Monomeric Aβ40 and Aβ42 is believed to have a fundamental role in this, forming both homogeneous and mixed aggregates (Gu & Guo 2013). Studies of CSF and plasma suggests that although Aβ40 is more abundant, it is also considered to be less toxic. Aβ42 on the other hand is more aggregation-prone and drives the formation of toxic insoluble oligomers and fibrils (Tiwari *et al.* 2019). It has also been reported that Aβ42 is most prominent and sometimes the only Aβ peptide in plaques (Gu & Guo 2013).

Research suggests that the accumulation of Aβ aggregates and plaques activates certain kinases such as GSK-3β and CDK5. These kinases are involved in abnormal phosphorylation of the tau protein, ultimately leading to the formation of NFTs. Activation of abnormal processes then further trigger events such as neuroinflammation, oxidative stress, disrupted synaptic signaling and mitochondrial dysfunction that drives neuronal damage and progressively leads to the impairments seen with AD (Azargoonjahromi 2024). Some of these events can be explained by the affect of plaques on the forebrain and hippocampal neurogenesis, leading to the loss of microglial cells and stimulation of neuronal stem cell senescence (Wang *et al.* 2016). Hippocampal neurogenesis is the generation of new neuronal cells, critical for cognitive function, memory processes and affective behaviours (Kempermann *et al.* 2015). Further, microglial cells play a pivotal role as the brain's macrophages, upholding homeostasis of the central nervous system (Pallarés-Moratalla & Bergers 2024). Senescence is triggered by events such as oxidative stress and DNA damage, causing the irreversible growth arrest of astroglial cells and thus disrupting homeostasis (Bhat *et al.* 2012).

While the cause of most AD cases is still unknown (Chen *et al.* 2017), research suggests that it can be familial or sporadic. Several mutations in familial AD has thus been identified as a factor in the amyloid hypothesis. Analysis of these mutations has revealed that they are often found close to the cleavage sites and could thus reduce cleavage efficiency, leading to an increased Aβ40/Aβ42 ratio (Chen *et al.* 2017) For example, the Flemish mutation cause a decrease in $\alpha$-secretase activity, leading to a 2-fold increase of Aβ40/Aβ42. Another example is the Swedish double mutation that affects $\beta$-secretase, leading to a 6-8 fold increase of Aβ peptide production compared to the wild-type APP. Other APP mutations include: E693Q (Dutch); E693K (Italian), E693G (Arctic), and D694N (Iowa). (MacLeod *et al.* 2015).

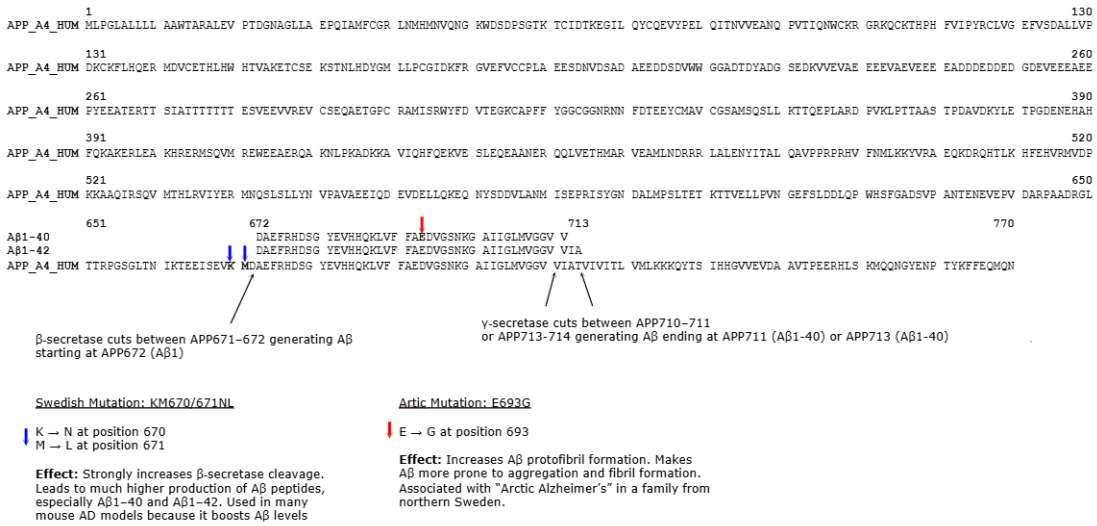


*Figure 2: Amino acid sequence of the human APP (amyloid precursor protein) including common cleavage and mutation sites. The illustration was created using Microsoft Powerpoint.*

In early onset, 65 and under, familial AD is predominant. However more than 90% of the cases are late-onset and considered to be sporadic (Piaceri *et al.* 2013). Regardless, the pathology of both types is reported to be very similar when looking at certain patterns (O'Brien & Wong 2011). One such example is the decrease in Aβ42 concentration of in the CSF, while still having unchanged Aβ40 concentrations (Alawode *et al.* 2022). Several studies has reported an increased risk of dementia with a lower ratio of Aβ40/Aβ42 in plasma (Fandos *et al.* 2017) and higher neurotoxicity related to an increased Aβ40/Aβ42 ratio in the brain. As a result, some studies have suggested that the Aβ40/Aβ42 ratio can be used to asses the accumulation of misfolded Aβ in the brain (Peng & Zhang 2021). Looking at the two in a relative ratio instead of their individual concentrations has shown to provide a more accurate representation of Aβ production (Alawode *et al.* 2022), offering an increased diagnostic accuracy (Baek *et al.* 2025).

While this is a promising method, it also comes with many challenges. Some studies report that the difference in peptides between healthy and AD affected individuals is low (Schöll *et al.* 2024). Others say that the peptides vary a lot in different parts of the brain, different individuals (Johansson *et al.* 2024) and that individuals under treatment for other medical conditions can have increased Aβ40/Aβ42 concentrations. For the Aβ40/Aβ42 ratio to be used as a trustworthy framework, it thus requires having a well-studied, accurate biomarker measurement approach (Schöll *et al.* 2024).

## 2.2 Antibodies

Antibodies (Abs) have come to be one of the most powerful tools within biological research due their high sensitivity and precision in identifying proteins (Ivell *et al.* 2014). Abs, or immunoglobulins (Ig), are Y-shaped proteins that are commonly divided into 5 isotypes: IgG, IgE, IgM, IgA and IgD (Chiu *et al.* 2019). The IgG antibody, with a total molecular weight of 150 kDa, is the most abundant isotype (Charles A Janeway *et al.* 2001). It consists, like the other isotypes, of two identical light chains (LC) and two identical heavy chains (HC) held together by disulfide bonds (Feldcamp & Carey 1996). The IgG can be divided into three main functional regions: fragment crystallizable (Fc), a hinge region and fragment antigen binding domains (Fabs). The most variable regions are found on the N-terminal of both LC and HC in the Fab region and are often referred to variable light (VL) and variable heavy (VH). In pairs, these regions make up two identical antigen binding sites, one on each arm of the ”Y”. (Chiu *et al.* 2019).

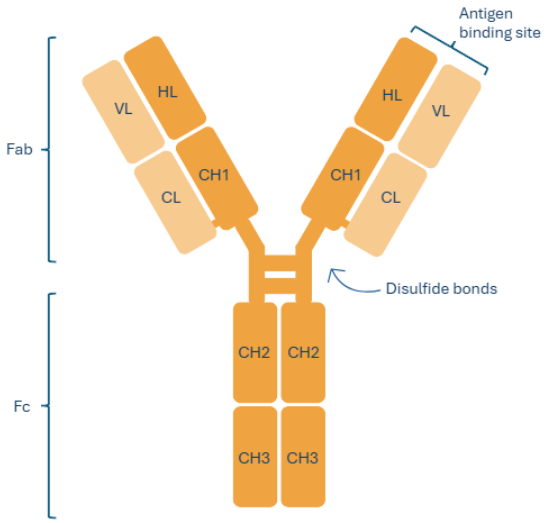


*Figure 3: Structure of an IgG1 antibody with light chains in light orange and heavy chains in dark orange. Fragment antigen binding domains (Fabs) and the fragment crystallizable (Fc) are illustrated using the brackets on the left. Variable domains and constant domains are given in VL/VH and CL/CH respectively. The illustration was created using Microsoft Powerpoint.*

Each binding site have a particular structure and conformation, these are called hyper-variable loops. These loops further make up the complementarity determining regions (CDRs) which shapes the unique binding site for the antigen, the paratope (Rojas 2022). The paratopes are made up of a selected number of amino acids (AAs) that often have aromatic side chains. Aromaticity has proven to be an important aspect of the antigen

recognition as the aromatic rings can bind favorably through several types of interactions depending on the complementary AA's on the antigen (Peng *et al.* 2014).

The complimentary AA's on the antigen are referred to as the epitope (Rojas 2022). They are often groups of surface-exposed AA side chains and can be classified as either linear or conformational, linear referring to a short peptide of continuous residues and conformational referring to several close residues that are not found in a continuous sequence (Viswanathan *et al.* 2024). Because of the complexity of antigens, and the numerous epitopes that they can have, the lymphocytes in the immune system produces different types of antibodies. Monoclonal antibodies are produced by a single clone of B lymphocyte cells and thus recognize single epitopes while polyclonal antibodies are produced by multiple clones and can recognize several epitopes (Lipman *et al.* 2005). Monoclonal antibodies have loads of applications within areas such as therapeutics and diagnostics. Since they can be directed towards very specific epitopes and produced in large quantities, they make terrific tools for identification and characterization in immunoassays (Siddiqui 2010).

However, when choosing a suitable antibody for recognition, its characteristics must be carefully considered. When working with aggregated proteins such as Aβ that have a structural complexity which can "hide" the epitopes, it is especially important to carefully select the capture and detection antibody to ensure strong and specific binding. (Metzendorf *et al.* 2025). Two common measures that are used when assessing antibody characteristics are specificity and affinity (Stapleton *et al.* 2005).

The specificity can be defined as the ability of an antibody to recognize an epitope in presence of other epitopes (Lipman *et al.* 2005). The specificity of the interaction is mainly affected by shape complementarity of the residues and chemical complementarity (Cavacini & Greenspan 2013). When there is a high degree of molecular shape complementarity, meaning the molecules "fit" well in presence of each other, more of the atoms can interact within energetically optimal distances and thus create more stable non-covalent interactions. (Greenspan 2023). The chemical complementarity also affect the energetics. For example, if the epitope is negatively charged and the paratope is positively charged, then there will be a greater complementarity and stronger binding (Cavacini & Greenspan 2013). Hydrogen bond donors and acceptors in close proximity is also likely to contribute this (Greenspan 2023).

The binding strength of an antibody to a single epitope is measured through affinity and the affinity constant. The affinity constant is derived from thermodynamics and it describes the amount of antibody-antigen complex that is formed at equilibrium. This means that an antibody with high affinity binds a larger amount of antigen in shorter time and with more stability than an antibody with low affinity (Lipman *et al.* 2005).

While it is often assumed that an antibody with high affinity also has high specificity, this is not always the case. An antibody with low affinity may be better at discriminating between two antigens, there is therefore no necessary link between them two. Choosing an antibody with high specificity could on the other hand result in less cross-reactivity (Lipman *et al.* 2005). While affinity is related to the relationship between an epitope and paratope, specificity is only relevant when there is several binding partners as it reflects the capacity of an Ab to react with several different antigens and discriminating between them (Van Regenmortel 2014).

The antibodies used in this project are 3D6 and RmAb158. 3D6 is a monoclonal IgG1 antibody that binds to the N-terminal region (AA 1-5) of monomeric and fibrillar Aβ, for both human and mice. Its humanized version and pharmaceutical is known as Bapineuzumab. RmAb158 is a monoclonal IgG2a antibody that binds large aggregates such as protofibrils and larger. It does however not bind that well to monomers and smaller oligomers. The pharmaceutical containing the humanized version of mAb158 is called Lecanemab (Metzendorf *et al.* 2025).

## 2.3 ELISA and Immunoassays

ELISA has its roots all the way back to the 1960s when the radio-immunoassay was introduced as a diagnostic tool by Rosalyn Yalow and Solomon Berson (Yalow & Berson 1960). In 1971, the ELISA immunoassay was introduced by Peter Perlmann, Eva Engvall, Anton Shuurs and Bauke van Weemen as a safer alternative (Engvall & Perlmann 1971) (Van Weemen & Schuurs 1971). Since its debut, it has become one of the most commonly used diagnostic tests in laboratories. Today, it is widely used to quantify proteins and other biomolecules as it offers fast, simple and accurate measurements of biological fluids (Aydin *et al.* 2025).

ELISA detects antigen-antibody binding through enzyme-labeled conjugates and substrates that result in color changes (Aydin *et al.* 2025). In medical diagnostics, a traditional optical sandwich ELISA is often performed on a 96-well plate where the capture antibody is already immobilized to the surface through physical absorption. It is also blocked to prevent non-specific binding of the antigen. The following steps involve addition of the antigen sample containing the biomolecule or biomarker of interest to the prepared 96-well plate. After incubation and formation of the antigen-antibody complex, excess antigen is washed away using a washing buffer and the enzyme-labeled detector antibody can be added to the plate. After additional incubation, the antibody-antigen-antibody complex is again washed before the addition of a color-generating enzyme substrate. The reaction is stopped through the addition of a stop solution and the

color change allows for measurement of absorbance, providing the concentration of the biomarker in the sample (Arya & Estrela 2018). There are also other versions of ELISA that use for example fluorescence or luminescence for detection (Gibbs 2012).

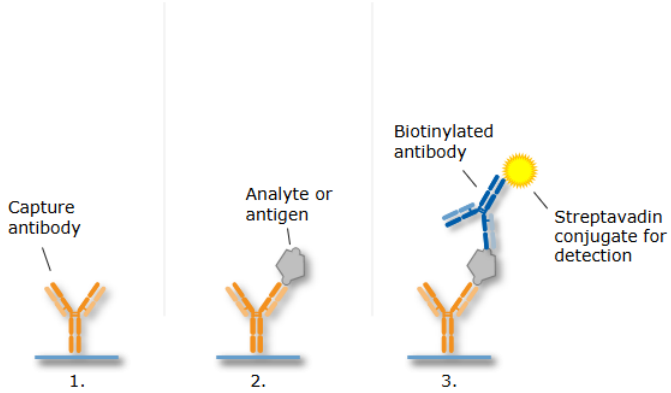


*Figure 4: Schematic drawing of a sandwich ELISA immunoassay. (1) Capture antibody is immobilized on a solid phase. (2) Antigen is captured by the capture antibody (3) Biotinylated antibody binds captured antigen. (4) Streptavadin-HRP conjugate and TMB substrate generate measurable color change. Original illustration from Cavidi AB, used with permission.*

There are many different variants of ELISA, therefore also large variation of the included components. As mentioned earlier, the antibodies are chosen with specificity to the antigen being detected for optimal signal generation. For example, to detect a biomarker in plasma, an anti-human IgG can be used as a detector antibody. The enzymes conjugated to the detector antibody is often alkaline phosphatase (AP) that uses BCIP/NBT (5-bromo-4-chloro-3-indolyl phosphate/nitro blue tetrazolium) as a substrate, or Horseradish peroxidase (HRP) that uses 3,3,5,5-Tetramethylbenzidine (TMB) as a substrate. When in presence of a peroxidase, TMB produces a blue color which becomes yellow when adding a stop solution, usually an acid such as HCl or $H_2SO_4$. (Aydin *et al.* 2025).

Signal generation is not only affected by the biological capture and detector components in the ELISA, there are several other factors that need to be carefully assessed. Materials such as type of assay plate, buffers and blocking agent can interfere with components and affect the signal (Zubair *et al.* 2026). One such example is non-specific binding of antigen or antibodies to the plate after the blocking step. This can create high background noise, which reduces the signal-to-noise ratio, affecting the accuracy and sensitivity of the analysis (Aydin *et al.* 2025).

Although the conventional ELISA offers many advantages, it is also limited. The detection limit for many tests do not reach below the nanomolar concentration of peptides.

This is an issue as many peptides are found in very low concentrations, especially in early stages of the disease (Arya & Estrela 2018). Consequently, there are several signal amplification methods that have been developed that aims to enhance the sensitivity and lower the limit of detection. Examples of such methods are electrochemiluminescence assays and single-molecule array, with many more methods emerging (Metzendorf *et al.* 2025). One such emerging method is BOLD.

## 2.4 Signal Amplification with BOLD

BOLD is a novel signal amplification technology that is the foundation of Cavidi's Exazym® technology. It allows researchers to measure a low abundance of biomolecules such as nucleic acids and proteins in biological samples that are otherwise difficult to detect using standard methods. The BOLD-technology is built upon a standard sandwich ELISA as it involves a capture antibody, antigen and detector antibody. What differs the BOLD-amplified ELISA from the standard ELISA is that the detector antibody has conjugated DNA-primers. In the Exazym® reaction, the primer-conjugated antibody is mixed together with a poly-rA template, BrdUTP and a polymerase with reverse transcriptase activity. This polymerase is then able to synthesize RNA/DNA hybrid strands using primer, BrdUTP and poly-rA template. The strands can then act as binding sites for multiple tertiary signal antibodies, amplifying the signal yield for each captured analyte (Cavidi 2024), (Cavidi 2025).

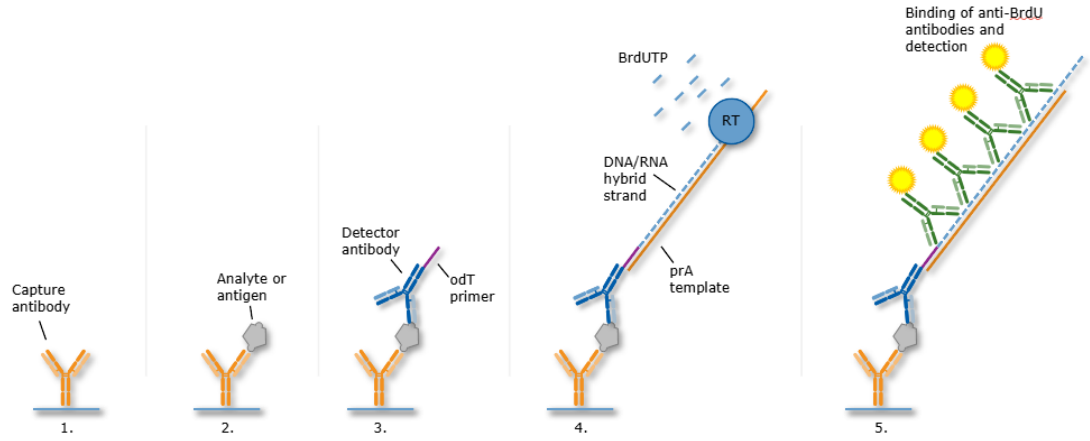


*Figure 5: Schematic drawing of the implementing the BOLD signal amplification technology in a sandwich ELISA.(1) Capture antibody is immobilized on a solid phase. (2) Antigen is captured by the capture antibody (3) OdT-primer labeled detector antibody binds to the captured antigen. (4) Reversed transcriptase (RT), prA template, and BrdUTP is added. RT synthesizes a complementary DNA strand, generating a DNA-RNA hybrid. (5) Multiple anti-BrdU antibodies bind to the hybrid. (6) Amplified signal is generated through the addition of Streptavadin-HRP and TMB substrate. Original illustration from Cavidi AB, used with permission.*

The conjugation of primers to the detector antibody is done using Click Chemistry. Click Chemistry is a group of reactions that are easy to apply, fast and versatile, making it a well used method within pharmaceutical sciences as it facilitates constructs with specific properties (Hein *et al.* 2008). The Click Chemistry approach for the conjugation is called Strain-promoted Azide-Alkyne Cycloaddition (SPAAC), a common conjugation tool used in chemical biology (Vidyakina *et al.* 2024). Broadly speaking, this involves labelling the antibody with azide ($-N_3$) tags and allowing the tags to react with the alkyne on the oligo-dT primer. In Exazym® terms this usually involves using a labelling the antibody using a NHS-PEG4-azide ClickChem label and later incubating the antibody together with a DBCO-TEG-OdT(30mer) primer (Cavidi 2025). What happens is that DBCO (dibenzocyclooctyne) is highly reactive towards 1,3-dipoles (azide) and the spontaneous reaction that occurs creates a stable 1,2,3-triazole. This reaction is ideal for bioconjugation it is a bioorthogonal reaction i.e there are no other reagents involved that might react with the biomolecule,(Debets *et al.* 2011).

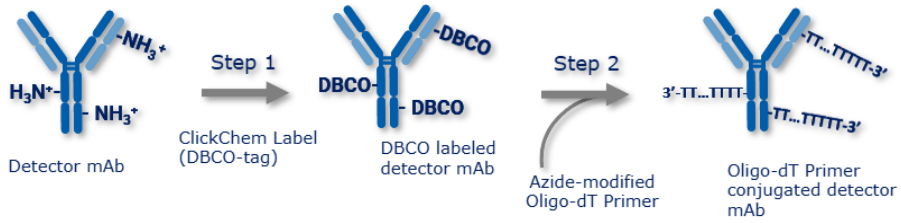


*Figure 6: Overview of the steps involved in the primer-antibody conjugation. Step 1: The antibody is conjugated with DBCO-modified ClickChem labels. Step 2: Azide-modified primer reacts with the labeled antibody creating a primer-conjugated antibody. Original illustration from Cavidi AB, used with permission.*

The ratio of Click Chemistry label and oligo-dT primer can be adjusted. Usually there is a 5-20 times molar excess of label relative the secondary antibody and a 5-20 times molar excess of the primer. This is to ensure that there is a significant signal amplification (Cavidi 2025). It is also possible to do the opposite configuration where the antibody is labeled with a DBCO-modified Click Chemistry label and the primer contains the azide. The this method of conjugation, written as ”Reverse” further on, is utilized in this project.

## 2.5 Precision and Reliability in Assay Development

When developing new methods, precision/reproducibility is crucial for the reliability of the assay. It ensures that potential variability in the results are due to biological differences in the sample and not inconsistencies in the method. It also ensures comparability

over time, that adjustments in the method actually make a difference and that the results are not just randomized. Generally, there are two types of reproducibility measures, intra-assay and inter-assay referring to reproducibility within the the same run and between runs. The precision is expressed through CV (%), coefficient of variation:
CV (%) = (standard deviation /mean) * 100 with a reliable method ideally being below 10% for intra-assay and below 15% for inter-assay (Schultheiss & Stanton 2009).

To estimate the sensitivity of the assay, there are typically two measures used to describe the smallest amount of an analyte that can be reliably measured in an assay: Limit of detection (LOD) and Lower limit of quantification (LLOQ). LOD is the lowest analyte concentration that can be distinguished from the background. It is usually determined by measuring around 10-20 replicates of a blank sample, calculating the mean and standard deviation (SD), and then calculating the LOD as: Mean + 2*SD. LLOQ is similar to LOD but it also has to meet certain demands about accuracy and precision. Similar to LOD, the LLOQ is therefore calculated using the mean and SD of blank sample values but with 10 SDs: Mean + 10*SD (Armbruster & Pry 2008).

# 3 Materials and Methods

## 3.1 Materials

### 3.1.1 Antibodies

The antibodies (3D6, RmAb158) used in this project were obtained from the Protein Drug Design group at the Department of Pharmacy, Uppsala University. Their characteristics are displayed in Table 1.

*Table 1: Characteristics of the of the antibodies used for capture and detection.*

| Antibody | Antibody type | MW (kDa) | Binding preference | Binding region |
|---|---|---|---|---|
| 3D6 | Murine monoclonal IgG1 | 147.4 | Monomers, aggregates | N-terminal, AA 1-5 |
| RmAb158 | Murine monoclonal IgG2a | 148.5 | Protofibrils | AA 3-8 |

### 3.1.2 Antigen

The antigens, Aβ40 monomers and Aβ42 protofibrils (Pf42) were also obtained from the Protein Drug Design group at the Department of Pharmacy, Uppsala University. They are human Aβ expressed in brain tissue from transgenic mouse models (tg-ArcSwe and tg-Swe). The Aβ40 and Aβ42 peptides are prepared by reconstituting lyophilized peptide in 10 mM NaOH to a concentration of 100 µM. The Aβ42 protofibrils are then formed through incubation of the Aβ42 peptide at 37°C, followed by; centrifugation and collection of the supernatant, and size-exclusion chromatography. For use in ELISA, the samples are then diluted in ELISa incubation buffer (1xPBS) (see Metzendorf *et al.* (2025) for further details).

### 3.1.3 Reagents

Specific details about the contents of the Exazym® reagents, such as Exazym® reaction solution, Exazym® polymerase buffer and Exazym® antibody buffer, will remain undisclosed to safeguard intellectual property.

## 3.2 Methods

### 3.2.1 Reverse ClickChem Conjugation of Detector Antibody

**STEP 1: Modification of the antibody with ClickChem label:** Freeze dried ClickChem label (DBCO-modified) was reconstituted to 100 mM by adding DMSO and further diluted to 0,5 mM through the addition of PBST (1xPBS + 0.05% Tween20) immediately before addition to the antibody. 0.5 mM DBCO label was added to antibody according to calculations (Sup Table 1) and incubated for 30 min. Quenching buffer (75 mM) and PBST was added to the samples to stop the reaction and incubated for 5 min. Uncoupled/deactivated DBCO labels were removed using spin columns. The spin column was equilibrated using PBST resulting in buffer exchange of the antibody into PBST and removal of excess DBCO-label following spin filtration.

**STEP 2: Conjugation of Oligo-dT Primer to the DBCO-modified Antibodies:** Freeze dried primer (azide-modified) was reconstituted to 210 µM by adding PBS. To all samples, primer dissolved in PBS was added (see Sup Table 1) and the samples were incubated at room temperature in dark overnight.

### 3.2.2 Micro BCA Assay

To estimate the concentration of the conjugated antibodies, a Micro BCA Protein Assay was performed using the Micro BCA Protein Assay Kit (Thermofisher Scientific #23212). Calculations for the calibration curve was prepared (Sup Table 2), and a working reagent was prepared to a ratio of 25:24:1 of reagents MA, MB and MC according to the protocol given with the kit. Antibody samples were also diluted 1:2 with PBST (1xPBS + 0.05% Tween20) in 1,5 mL Protein LB Microtubes (Sarstedt, 72.706.600). In 200µL PCR-vials, sample/standard point and working reagent were then prepared in a 1:1 ratio followed by incubation at 37°C in a waterbath for 120 min. Samples were then cooled and spun down before the absorbance measurement at 562 nm. Each calibrator and sample was done in triplicates and measured individually. The calibration curve was illustrated using a 4PL model and sample absorbances were interpolated into concentrations using Python. Sample dilutions were compensated in the calculations.

Code for the 4PL model was generated using ChatGPT (OpenAI 2025) based on code written by Rob Harrand (Harrand 2023). For details, see Appendix, section A.1.

### 3.2.3 SDS PAGE

For analysis of the conjugated antibodies, an SDS-PAGE was performed. 1x running buffer was prepared using 10x Tris/Glycine/SDS buffer (Bio-Rad, #1610732). A Mini-PROTEAN TGX stain-free 4-15% gel (Bio-Rad, #456-8085) was prepared and the wells were rinsed with 1X running buffer before being assembled into the electrophoresis cell. Samples, each containing 5µg of antibody, were prepared with 4X Laemmli sample buffer (Bio-Rad, #1610747) + 200 mM DTT (Bio-Rad, #1610610) and denatured for 15 min at 95°C. Samples were then cooled for 10 min at 4°C, spun down and applied to the gel, 20µL per sample or 5 µL Precision Plus Kaleidoscope standards (Bio-Rad, #1610375) in separate wells. The gel was run at 200 V for 35 min followed by fixation for 15 min using 40% EtOH/10% acetic acid. The gel was rinsed with dH2O and stained overnight with a slight shake using QC Colloidal Coomassie Stain (Bio-Rad, #1610803). The gel was rinsed and destained using dH2O before gel imaging.

### 3.2.4 Biotinylation of Detector Antibodies for the Standard ELISA

Antibodies 3D6 and RmAb158 were biotinylated using the EZ-Link Sulfo-NHS-Biotin (Thermo Scientific, #A39256). Before the procedure, a 1 mg vial containing EZ-Link Sulfo-NHS-Biotin was removed from the freezer and brought to room temperature before being reconstituted to 10 mM using ultrapure water. This was done immediately before use as the NHS-ester hydrolyzes and becomes non-reactive if left for too long in water. Before being added to the antibodies, the biotin was diluted to 1 mM to get a better working volume. Both antibodies were diluted to a concentration of 1.07 mg/mL and a volume of 50 µL. Calculations of appropriate volumes of biotin were done according to the formulas given in the kit protocol. The antibody-biotin solution was then incubated while shaking on a plate shaker for 30 min in room temperature. To reach a final volume of 80 µL needed for the spin columns PBS was added after incubation. The spin column was equilibrated using PBS resulting in buffer exchange of the antibody into PBS and removal of excess biotin following spin filtration.

### 3.2.5 Direct ELISA for Confirmation of Successful Biotinylation

To ensure that the biotinylation of the 3D6 and RmAb158 detector antibodies did not interfere with the antigen binding, they were tested in a direct ELISA. Both antibodies in concentrations ranging from 6.4 µg/mL - 0.0064 µg/mL were directly immobilized to a transparent 96-well plate (Thermofisher Scientific, #445101) and incubated for 120 min at 37°C. The plate was washed using wash buffer (PBS + 0.05% Tween 20) in a Tecan hydraflex with the Maxi10 setting (400 µL x 3) and coated with Blocker™ Casein in PBS (Thermofisher Scientific, #37528). The plate was incubated for 60 min

at RT followed by coating with SA-HRP (R&D Systems, #DY998) diluted 1:200 in dilution buffer and incubated for 60 min at room temperature (abbreviated RT, 20-25°C) . Subsequently, 1-Step TMB ELISA substrate (Thermofisher Scientific, #34028) was added to the plate and incubated for 30 min in dark at RT. The reaction was stopped by addition of $1MH_2SO_4$ and absorbance was measured at 450 nm using a Tecan Spark Microplate reader. Between each incubation step, plates were washed using Maxi10 (400 µL x 3) using wash buffer unless stated otherwise.

### 3.2.6 Capture and Detector Antibodies

Capture antibodies and detector antibodies used in the standard ELISA and BOLD-amplified ELISA are displayed in Table 2.

*Table 2: Capture and detector antibodies used in the project. For the conjugated detector antibodies used in the BOLD-amplified assay, the ratio of ClickChem label:Primer is displayed in brackets.*

| Capture antibody | BOLD detector antibody | Standard detector antibody |
|---|---|---|
| 3D6 | 3D6 (5:5)<br>3D6 (20:5) | Biotinylated 3D6 |
| RmAb158 | RmAb158 (5:5)<br>RmAb158 (20:5) | Biotinylated RmAb158 |

### 3.2.7 Standard ELISA Protocol

The standard ELISA was performed in addition to the BOLD-amplified ELISA as a comparative measure. This was done according to the following protocol:

Capture antibody diluted in PBS to a concentration of 1 µg/mL was immobilized to a transparent 96-well plate (Thermofisher Scientific, #445101) and incubated overnight at 4°C. The plate was washed using wash buffer (PBS + 0.05% Tween 20 in a Tecan hydraflex with the Maxi10 setting (400 µL x 3). Subsequently, the plate was blocked using Blocker™ Casein in PBS (Thermofisher Scientific, #37528) for 2h at RT to block the surface. After removal of the blocking solution, a calibration curve was generated using serial dilutions of antigen (Aβ40/Pf42) in dilution buffer (PBST + 0.1% Casein). The calibration curve covered the range of 4.12 - 1000 nM/pM across seven calibrator points generated by 3-fold serial dilutions from stock 100µM/5µM, with all calibrators analyzed in duplicates. The plate was coated with the calibration curve and incubated overnight at 4°C. Further, the plate was coated with 1 µg/mL biotinylated detector antibody diluted in dilution buffer and incubated for 3h at RT. This was further followed by dilution 1:200 of SA-HRP (R&D Systems, #DY998) in dilution buffer and incubation for 60 min at RT. To generate the colored reaction, 1-Step TMB ELISA substrate (Ther-

mofisher Scientific, #34028) was added to the plate and incubated for 30 min in dark at RT. The reaction was stopped by addition of 2M $H_2SO_4$ and absorbance was measured at 450 nm using a Tecan Spark. Between each incubation step, plates were washed using Maxi10 (400 µL x 3) using wash buffer unless stated otherwise.

### 3.2.8 BOLD-amplified Standard ELISA Protocol

Capture antibody diluted in PBS to a concentration of 1 µg/mL was immobilized to a transparent 96-well plate (Thermofisher Scientific, #445101) and incubated overnight at 4°C. The plate was washed using wash buffer (PBS + 0.05% Tween 20) in a Tecan hydraflex with the Maxi10 setting (400 µL x 3). Subsequently, the plate was blocked using Blocker™ Casein in PBS (Thermofisher Scientific, #37528) for 2h at RT to block the surface. After removal of the blocking solution, a calibration curve was generated using serial dilutions of antigen (Aβ40/Pf42) in dilution buffer (PBST + 0.1% Casein). The calibration curve covered the range of 4.12 - 1000 nM/pM across seven calibrator points generated by 3-fold serial dilutions from 100µM/5µM, with all calibrators analyzed in duplicates. The plate was coated with the calibration curve and incubated overnight at 4°C. The steps until this point are the same as for the standard ELISA. The following steps are specific for the BOLD-amplified format: The plate was coated with reverse-conjugated detector antibody diluted in dilution buffer (PBST + 0.1% Casein) and incubated for 3h at RT. Exazym® Reaction Solution (RS) mixed with poly-rA (22 µL per mL) and Polymerase diluted in Exazym® Polymerase Buffer to a concentration of 0.65 U/mL were prepared and added to the plate (23 µL + 77 µL). The plate was incubated for 30 min incubation at RT before being coated with Exazym® Biotin Antibody (biotinylated anti-BrdU mAb) diluted in Exazym® Antibody buffer to a concentration of 0.3 µg/mL. This was again incubated for 30 min at RT, followed by coating with SA-HRP diluted 1:200 in dilution buffer and incubation for 60 min at RT. The last steps involved the addition of TMB substrate and incubation for 30 min before adding stop solution, $H_2SO_4$. Absorbance was measured at 450 nm. Between each incubation step, plates were washed using Maxi10 (400 µL x 3) using wash buffer unless stated otherwise.

### 3.2.9 Optimized Final BOLD-amplified Standard ELISA Protocol

The optimized BOLD-amplified standard ELISA format used shortened incubation times and adjusted reagent concentrations to reduce non-specific binding, thereby lowering background noise.

RmAb158 capture antibody diluted in PBS to a concentration of 1 µg/mL was immobilized to a transparent 96-well plate (Thermofisher Scientific, #445101) and incubated

overnight at 4°C The plate was washed using wash buffer (PBST) in Tecan hydraflex with the Maxi11 setting (400 µL x 8). Post-wash, the plate was blocked using 2% BSA in PBS for 120 min at RT. After removal of the blocking solution, a calibration curve was generated using serial dilutions of Pf42 in dilution buffer (PBST + 0.1% Casein). The calibration curve covered the range of 4.12 - 1000 pM across seven calibrator points generated by 3-fold serial dilutions from 5µM, with all calibrators analyzed in duplicates. The plate was coated with the calibration curve and incubated overnight at 4°C. The plate was coated with 0.1 µg/mL 3D6 5:5 reverse-conjugated detector antibody diluted in dilution buffer (PBST + 0.5% Casein) and incubated for 60 min at RT. Exazym® Reaction Solution (RS) mixed with poly-rA (22 µL per mL) and Polymerase diluted in Exazym® Polymerase Buffer to a concentration of 0.65 U/mL were prepared and added to the plate (23 µL + 77µL). The plate was incubated for 30 min at RT before being coated with Exazym® Biotin Antibody (biotinylated anti-BrdU mAb) diluted in Exazym® Antibody buffer to a concentration of 0.3 µg/mL. This was again incubated for 30 min in RT, followed by coating with SA-HRP diluted 1:200 in dilution buffer and incubation for 30 min at RT. The last steps involved the addition of TMB substrate and a 30 min incubation before adding stop solution, $H_2SO_4$. Absorbance was measured at 450 nm. Between each incubation step, plates were washed 8 times using wash buffer with the exception of a 3x wash after the blocking step to preserve the binding of blocking agent to the plate and prevent non-specific binding of subsequent reagents.

### 3.2.10 Statistics and Analysis of Absorbance Data

Analysis of the absorbance data obtained from the 450 nm measurements were performed using the Microsoft Excel application, this includes generation of figures. To ensure precision and reproducibility, each calibrator were measured in duplicate wells using the same solution.

Code for the 4PL model used for the precision analysis was generated using ChatGPT (OpenAI 2026)and ClaudeAI (Anthropic 2026) based on the code from the µBCA. For details, see Appendix, section A.2.

# 4 Results

## 4.1 Validation and Quantification of Reverse-conjugated Oligo-dT Detector Antibodies and Biotinylated Detector Antibodies

Antibodies 3D6 and RmAb158 was subjected to primer-conjugation using Reverse Click Chemistry for their use as detector antibodies in the BOLD ELISA assay. The detector antibodies were named based on their ratio of DBCO-label and Azide-primer (label:primer). Concentrations for the antibody conjugates 3D6 5:5, 3D6 20:5, RmAb158 5:5 and Rmab158 20:5 were 239 µg/mL, 285 µg/mL, 288 µg/mL and 306 µg/mL respectively, estimated using µBCA and a 4PL model (see Sup Tables 2 and 3).

SDS-PAGE was used to verify successful conjugations and asses conjugation levels through molecular weight using unconjugated 3D6 and RmAb158 as negative control samples. Results from the SDS-PAGE can be seen in Figure 7 illustrating successful conjugations for both antibodies with an increased number of observable bands for the light chain (25 kDa) and the heavy chain (50 kDa). The conjugation performed with a higher molar excess of primer to ClickChem label (20:5 vs 5:5) is more smeared, illustrating a larger variation of conjugates with more primer conjugated to the heavy chain. However, there is still strong bands for the light and heavy chains for both conjugates, suggesting that there are also unmodified antibodies in the sample. Although the SDS-PAGE can be used to assess if the conjugation was successful, it can not reveal anything regarding where on each chain the conjugation has occurred and if it affects antibody-antigen binding.

For the standard ELISA assay, the 3D6 and RmAb158 detector antibodies were biotinylated. Concentrations were estimated using absorbance (280 nm) before and after conjugation resulting in final concentrations of 628 µg/mL for 3D6 Biotin and 743 µg/mL for RmAb158 Biotin (See Sup Table 6). A direct ELISA was also performed to ensure that the biotinylation had been successful without interfering with the Pf42 binding site. The evaluation was done using two previously confirmed biotinylated antibodies as positive controls. The absorbance measurement showed high signals for both antibodies confirming binding to the Pf42 antigen (See Sup Table 7).

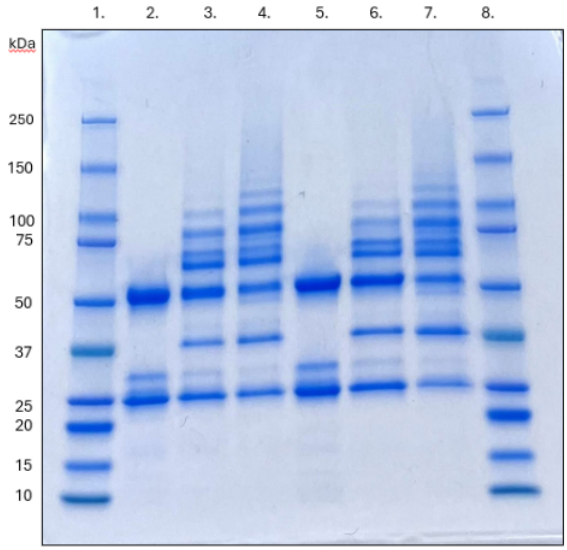


*Figure 7: Analysis of conjugated antibodies on a 4–15% precast polyacrylamide gel. All antibodies were analyzed at an amount of 5 µg and under reducing conditions. Lane 1: 5 µL Precision Plus Protein™ Kaleidoscope™ Prestained Protein Standards. Lane 2: 3D6, Lane 3: 3D6-odT30mer (5:5), Lane 4: 3D6-odT30mer (20:20), Lane 5: RmAb158, Lane 6: RmAb158-odT30mer (5:5), Lane 7: RmAb158-odT30mer (20:5), Lane 8: 5 µL Precision Plus Protein™ Kaleidoscope™ Prestained Protein Standards. Expected bands at 25 kDa and 50 kDa for unconjugated light and heavy chains respectively. Expected bands at >25 kDa and >50 kDa for primer-conjugated light and heavy chains.*

## 4.2 Evaluation of Antigen, Capture and Detector Antibody

The Click Chemistry conjugation of the detector antibodies 3D6 and RmAb158 resulted two different ratios of label:primer, these were 5:5 and 20:5. The idea is that antibodies with higher ratio ClickChem label have more available, reactive groups that can react with the free primer. This would in hypothesis increase the number of primers on the antibody and result in greater signal generation during the BOLD reaction. This hypothesis was investigated by testing the four detector antibody conjugates abilities to bind monomeric Aβ40 and Pf42. Absorbance measurements from the BOLD-amplified assays using RmAb158 as capture antibody illustrated great signal generation with all conjugates. Conjugates with ratio 20:5 did however display a larger background noise than the 5:5 conjugates, likely due to non-specific binding, without a significant gain in signal (see Figure 8). As a low signal-to-noise ratio is essential for signal evaluation, the 5:5 conjugates were utilized in the subsequent BOLD-amplified assays.

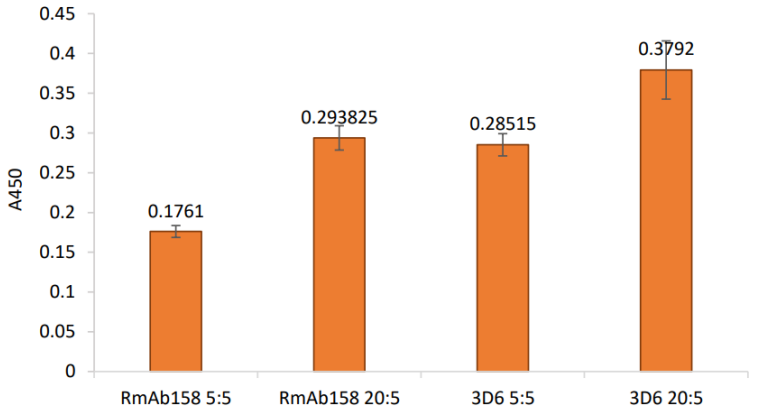


*(a) Mean (n=2) background absorbance (450nm) values*

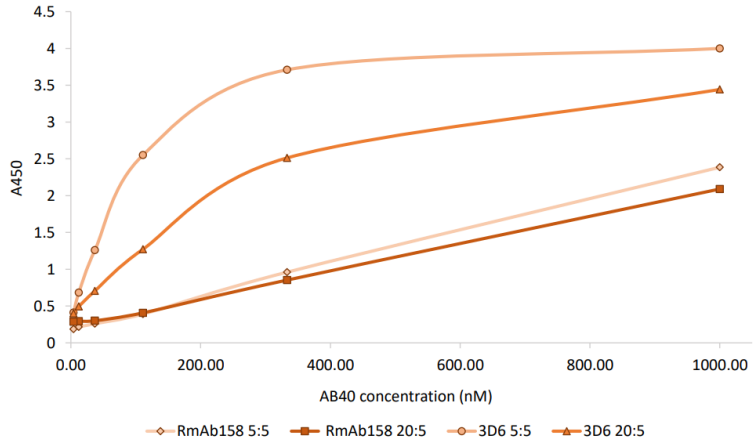


*(b) Mean (n=2) absorbance (450nm) values*

*Figure 8: Obtained mean background noise and calibration curves from the RmAb158 capture antibody assay used to determine the performance of each OdT-detector conjugate. The antigen sample used in this assay was Aβ40 monomers in concentrations 4.12 - 1000 nM.*

3D6 as a capture antibody in the BOLD-amplified assay has throughout the performed experiments consistently showed high, elevated background noise (see Figure 9a for representative example). Even with adjustments of the assay components such as a 20x reduction of the detector antibody concentration, these issues remained. Background issues has not been present in the standard ELISA to the same extent, suggesting underlying issues with the antibody or the standard assay in itself that is amplified when used with BOLD. Although the BOLD-amplified assay with RmAb158 as capture antibody also displayed background issues, the signal-to-noise ratio was interpretable. The majority of the BOLD-amplified assays has thus been performed using RmAb158 where adjustments has been made to lower background noise.

| Antigen conc (pM) | 3D6 capt + RmAb 5:5 0.25 µg/mL | 3D6 capt + 3D6 5:5 0.25 µg/mL | 3D6 capt + RmAb biot 2 µg/mL | 3D6 capt + 3D6 biot 1µg/mL |
|---|---|---|---|---|
| 10000 | OVER | OVER | 0.57055 | 2.86835 |
| 3333.3 | OVER | OVER | 0.15225 | 1.0468 |
| 1111.1 | OVER | OVER | 0.092 | 0.5564 |
| 370.4 | OVER | OVER | 0.07985 | 0.3414 |
| 123.5 | OVER | OVER | 0.0735 | 0.2793 |
| 41.2 | OVER | OVER | 0.0697 | 0.2625 |
| Blank | OVER | OVER | 0.06995 | 0.2476 |
| Blank | OVER | OVER | 0.0708 | 0.24545 |

*(a) 3D6 capture antibody assay*

| Antigen conc (pM) | RmAb capt + RmAb 5:5 0.25 µg/mL | RmAb capt + 3D6 5:5 0.25 µg/mL | RmAb capt + RmAb biot 2 µg/mL | RmAb capt + 3D6 biot 1µg/mL |
|---|---|---|---|---|
| 10000 | OVER | OVER | 1.48575 | 3.4847 |
| 3333.3 | OVER | OVER | 0.5636 | 1.7393 |
| 1111.1 | 3.8841 | OVER | 0.2582 | 0.80035 |
| 370.4 | 2.9817 | 3.8471 | 0.1377 | 0.4633 |
| 123.5 | 2.2778 | 3.14455 | 0.0979 | 0.3348 |
| 41.2 | 2.11785 | 2.53115 | 0.09005 | 0.2831 |
| Blank | 1.75605 | 2.003 | 0.07615 | 0.24765 |
| Blank | 2.19915 | 2.59935 | 0.07865 | 0.26355 |

*(b) RmAb158 capture antibody assay*

*Figure 9: Obtained mean (n=2) absorbance (450 nm) data from two comparative assays used to evaluate the performance of capture antibodies 3D6 and RmAb158 using Pf42 antigen (a) Mean OD450 from using 3D6 1 µg/mL as capture antibody with BOLD (green) and without BOLD in a standard ELISA (yellow) (b) Mean OD450 from using RmAb158 1 µg/mL as capture antibody with BOLD (green) and without BOLD in a standard ELISA (yellow).*

Initially the project focused on the detection of Aβ40 monomers as previous attempts had been done using protofibrils, this did however prove to be difficult as detection required the antigen calibration curve to be in the nanomolar range (4.12 nM - 1 µM). The results (Figure 8) does however suggest that there indeed is some binding of RmAb158 as there is signal generation in the BOLD-amplified assay that has not previously been seen in the standard ELISA assay. A prerequisite for a sandwich ELISA to work is that the capture antibody and the detector antibody both have affinity for the antigen, otherwise no signal would be generated. This was however not further investigated in this project due to time constraints, instead another antigen sample containing Aβ42 protofibrils (Pf42) was tested. The Pf42 samples were possible to detect in the picomolar range for both the standard assay and the BOLD-amplified assay. Sensitivity for the lower ranges of Aβ is important for this type of assay since the concentrations of Aβ in plasma is generally very low. The Pf42 sample is thus used in all results presented further in this section unless stated otherwise.

## 4.3 Evaluation of Background Noise Reduction Strategies in the BOLD-amplified ELISA

The BOLD-amplified standard ELISA protocol has been used as the starting protocol. As the standard ELISA assay has been used as a comparative measure, this protocol is very similar in terms of antibody concentrations and incubation times with the addition of the BOLD steps. There is however no adjustments to the signal amplification given with BOLD.

To optimize the BOLD assay performance, several experimental assay parameters were evaluated including detector antibody concentrations, blocking buffers, antigen/detector antibody diluents and incubation times etc. These experimental screenings collectively aimed to identify the conditions that maximize signal generation and minimize background noise, effectively increasing the signal-to-noise ratio (SNR). As the optimization has been an iterative process, certain screenings has been repeated several times after adjustments of previously tested parameters. This was done to ensure that the resulting assay conditions were non-biased. The evaluated and selected conditions are displayed in Table 3 below.

*Table 3: Table depicting the evaluated assay parameters, the evaluated conditions for each parameter and the selected condition based on the results from the assay parameter screening.*

| Assay parameter | Evaluated conditions | Selected condition |
|---|---|---|
| Capture Antibody | 3D6, RmAb158 | RmAb158 |
| Detector Antibody | 3D6 5:5, 3D6 20:5, RmAb158 5:5, RmAb158 20:5 | 3D6 5:5 |
| Detector Antibody concentration | 0.05 µg/mL, 0.1 µg/mL, 0.2 µg/mL | 0.1 µg/mL |
| Capture Antibody incub time | Overnight at 4°C, 120 min at 37°C | Overnight 4°C |
| Antigen incub time | Overnight at 4°C, 120 min at RT, 60 min at RT | Overnight 4°C |
| Detector antibody incub time | 180 min, 120 min, 60 min | 60 min |
| Blocking agent | 1% Casein in PBS, 2% BSA in PBS, RIA buffer | 2% BSA in PBS |
| Antigen diluent | 0.5% Casein in PBST, 1% BSA in PBST, RIA buffer | 1% BSA in PBST |
| Detector diluent | 0.5% Casein in PBST, 1% BSA in PBST, RIA buffer | 0.5% Casein in PBST |

### 4.3.1 Incubation Time

Reduction of background noise is a recurring challenge with assay development which is often a result of non-specific binding. Incubation time is a parameter with great impact on binding capacity, directly affecting the amount of non-specific binding in a certain assay. Since the BOLD-amplified assay starting protocol is based on the standard ELISA protocol it uses long incubation times in certain steps. Shorter formats of the protocol were therefore tested to investigate if that would improve the SNR. Specifically, the capture antibody, detector antibody and SA-HRP incubation times were modified in two assays, one for each detector antibody 3D6 5:5 and RmAb158 5:5. Both assays displayed very similar background noise but the 3D6 detector antibody assay gave overall higher signals. As a representative illustration, the results from the modifications in the 3D6 5:5 detector antibody assay is presented in Figure 10 and 11.

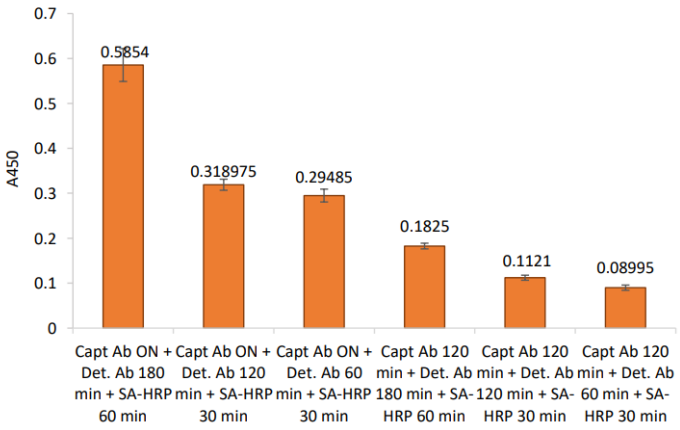


*Figure 10: Mean (n=2) absorbance (450 nm) background noise obtained during optimization of capture antibody and detector antibody incubation times in the BOLD-amplified ELISA. The RmAb158 capture antibody was applied in a 1 µg/mL concentration and the 3D6 5:5 OdT-detector antibody in a concentration of 0.05 µg/mL. Error bars represent the standard deviation.*

As seen in Figure 10, there is a clear decrease in background noise when using a shorter format of the protocol. Reducing the detector antibody incubation time by 1 hour and the SA-HRP incubation time by 30 min decreases the background by half. When further reducing the capture antibody incubation from overnight at 4°C to 2h in 37 °C, the noise is reduced even more. Although the background noise are reduced, the obtained mean OD values presented in Figure 11a suggests that the shorter protocol formats also result in lower signal generation of Pf42-specific signals. The SNR, seen in Figure 11b, on the other hand suggest that the reduction of background noise exceeds the reduction of signal for concentrations above 150 pM. For concentrations below 150 pM the SNR stays consistent throughout all protocol formats suggesting that the overall sensitivity for the assay has not changed.

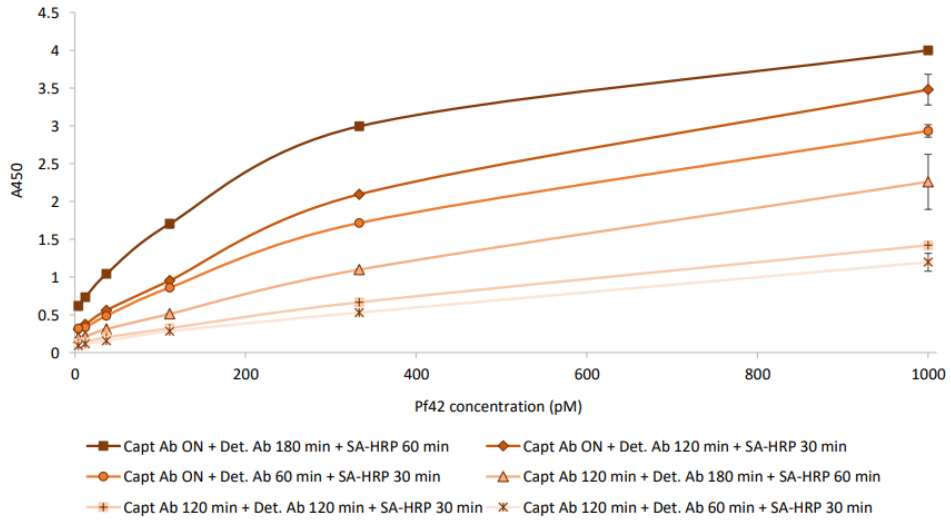


*(a) Mean OD450*

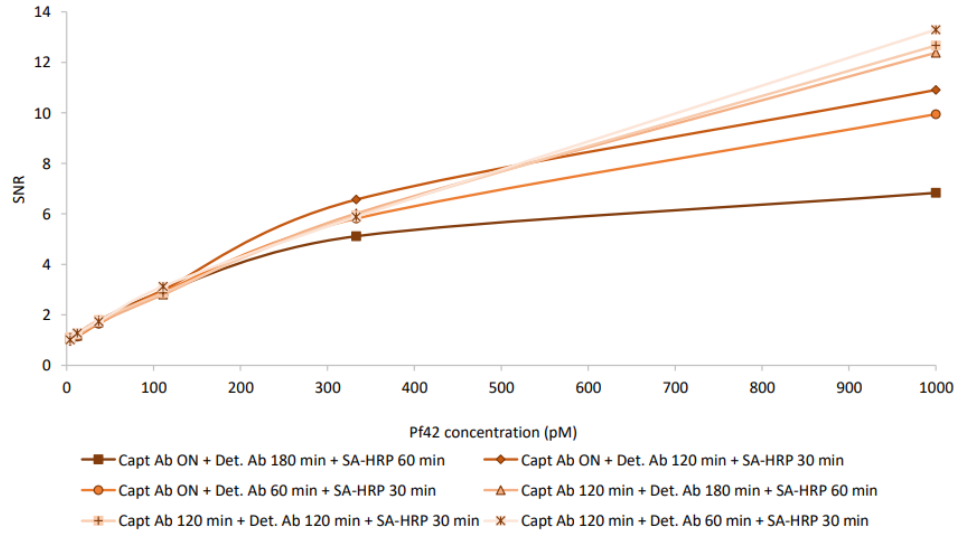


*(b) SNR*

*Figure 11: (a) Calibration curves of the mean (n=2) absorbance (OD450) values obtained during optimization of capture antibody and detector antibody incubation times in the BOLD-amplified ELISA. The RmAb158 capture antibody was applied in a 1 µg/mL concentration and the 3D6 5:5 OdT-detector antibody in a concentration of 0.05 µg/mL. Each graph represents the obtained OD-values for Pf42 concentrations 4.12 -1000 pM under the specified conditions. Error bars represent the standard deviation (b) Signal-to-noise ratio as a function of Pf42 antigen concentrations 4.12-1000 pM used to determine the optimal capture and detector antibody incubation time.*

As a shorter capture antibody incubation time did not change the SNR for the lower concentrations, the overnight incubation was continued for the following experiments. The detector antibody incubation time and the SA-HRP incubation time was however

reduced from 180 min + 60 min to 60 min + 30 min as this reduced the background noise and shortened the overall protocol, yielding faster results.

In the early testing of the assay, monomeric Aβ40 was detected using a RmAb158-coated plate, something that in theory should not happen as the RmAb158 antibody allegedly only has affinity to larger aggregates and protofibrils. A hypothesis to why signal generation was still possible is that the antigen aggregates during the incubation process. Aggregation during the incubation process of the assay would not be ideal as that could misrepresent the true form of Aβ. The initial BOLD-amplified standard ELISA protocol uses an overnight antigen coating. To prevent aggregation it would be better to have a shorter incubation period but without loosing signal. To investigate if a shorter Pf42 incubation had any affect on the signal, two incubation times, 120 min and 60 min both in RT, were tested and compared towards the overnight 4°C incubation.

Figure 12 illustrates that there is a clear loss in signal when reducing the antigen incubation time. The antigen likely requires a longer incubation step to properly bind the capture antibody. Other measures would have to be investigated to prevent additional aggregation. An important note is that in this screening the capture antibody was incubated for 120 min at 37°C, not overnight. This could have affected the binding of the antigen and lowered the signals overall.

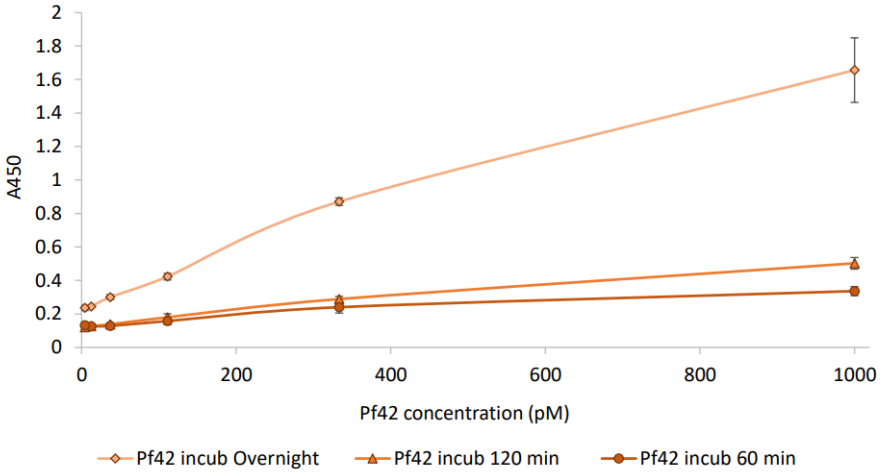


*Figure 12: Calibration curves of the mean (n=2) absorbance (OD450) values obtained during the evaluation of Pf42 incubation time in the BOLD-amplified ELISA. The RmAb158 capture antibody was applied in a 1 µg/mL concentration and incubated for 120 min (not overnight) and the 3D6 5:5 OdT-detector antibody at 0.05 µg/mL. Error bars represent the standard deviation.*

### 4.3.2 Blocking Buffers and Diluents

Changing the blocking buffers and dilution buffers, is another way of targeting the background noise issue. The blocking step after the capture antibody incubation and the use of blocking agents in the dilution buffer used with antigen and detector antibodies is meant to reduce non-specific binding. However not all blocking agents are equally compatible with all reagents. To find the optimal blocking agent for each step of the assay, different combinations of Casein and BSA were evaluated (see Sup Figure 5). For the blocking step after the capture antibody immobilization, three blocking buffers were evaluated: 1% Casein in PBS, 2% BSA in PBS and RIA buffer. The RIA buffer contains 1% BSA along with detergents that aims to lower background noise (see Supplementary methods for buffer reagents). The same blocking agents were used in diluents for Pf42 antigen, the detector antibody and the SA-HRP with Tween20: PBST + 0.5% Casein, PBST + 1% BSA and RIA buffer. The RIA buffer was not used as diluent for the antigen as the detergents might affect the structural integrity of the protein.

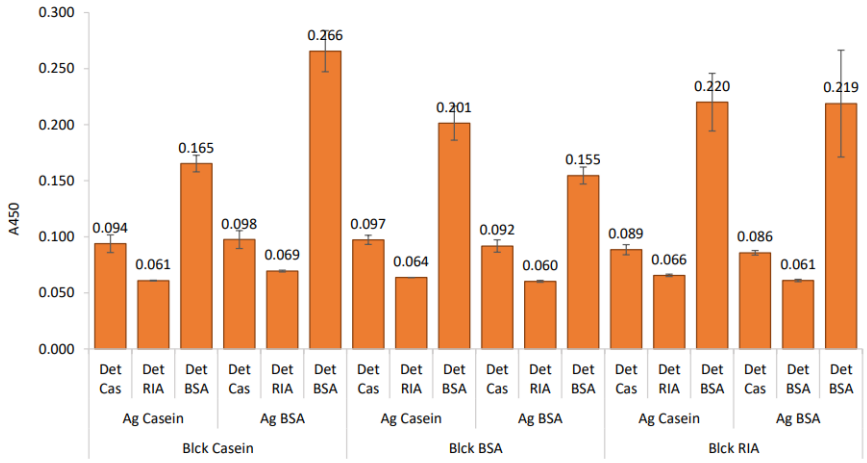


*Figure 13: Mean (n=2) absorbance (450 nm) background noise obtained during optimization of blocking buffers and dilution buffers in the BOLD-amplified ELISA. The RmAb158 capture antibody was applied in a 1 µg/mL concentration and the 3D6 5:5 OdT-detector antibody in a concentration of 0.05 µg/mL. Error bars represent the standard deviation.*

As seen in Figure 13, the different blocker combinations had a significant reducing effect on the background noise. What becomes evident is that when the RIA buffer is used as detector diluent, the obtained background noise very low, regardless of what blocking agents were used in the previous steps. Using 1% BSA in PBST as detector diluent displayed the opposite overall showing almost double the background compared to RIA and 0.5% Casein in PBST as diluents.

Although the samples with RIA buffer diluent displayed low background noise they

also displayed very low Pf42 specific signals as seen in Figure 14. BSA and Casein as detector antibody diluent showed relatively similar results in regard to the SNR. Pf42 antigen diluted in BSA diluent showed better overall Pf42 specific signals than samples with Casein.

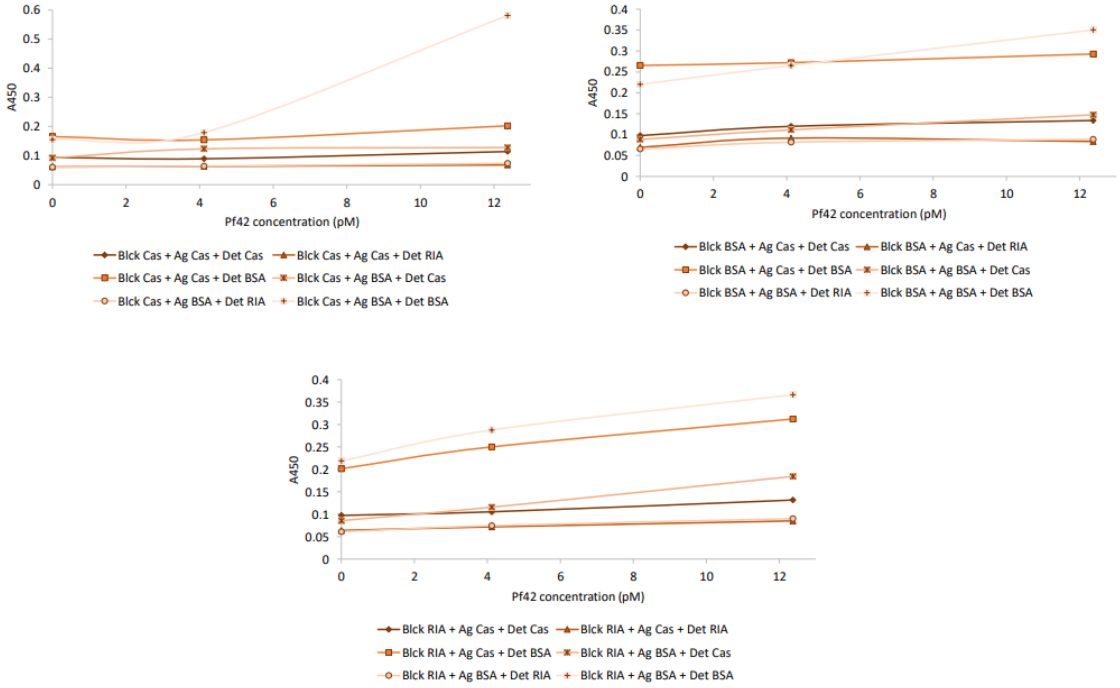


*Figure 14: Raw absorbance (450 nm) background noise obtained during optimization of blocking buffers and dilution buffers in the BOLD-amplified ELISA. Each combination is noted as: Blocking buffer + Antigen diluent + Detector diluent.*

As several combinations of blocking buffers and antigen/antibody diluents showed promising results, three were chosen to investigate further in the evaluation of detector antibody concentration to see if the Pf42 signals could be increased. The chosen combinations were the following:

1. Blocking PBS + 1% Casein | Antigen diluent PBST + 1% BSA | Detector diluent PBST + 1% BSA
2. Blocking PBS + 2% BSA | Antigen diluent PBST + 1% BSA | Detector diluent PBST + 0.5% Casein
3. Blocking RIA buffer | Antigen diluent PBST + 1% BSA | Detector diluent PBST + 0.5% Casein

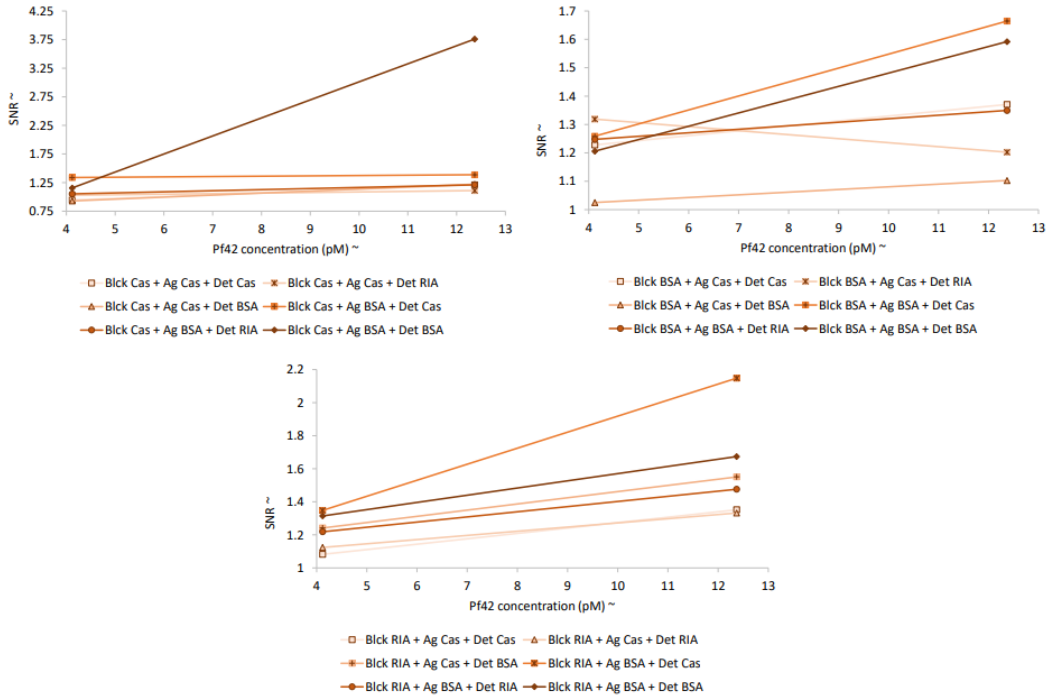


*Figure 15: Signal-to-noise ratio as a function of Pf42 antigen concentrations 4.12-1000 pM used to determine the optimal blocking and dilution buffers. Each combination is noted as: Blocking buffer + Antigen diluent + Detector diluent.*

To further decrease the background noise from previous screenings, the washing steps were increased. Instead of 3x400µL, all wash steps were increased to 8x400 µL except the wash after blocking of the capture antibody. This 3x400 µL wash was kept to ensure that sufficient protein remains to prevent non-specific binding to the plate.

### 4.3.3 Detector Antibody Concentrations

In the evaluation of blocking buffers and antigen/antibody diluents, a low concentration of the detector antibody was used resulting in low Pf42-specific signal values. Hence, it was of interest to investigate what effect an increase in concentration would have on the SNR. Three combinations of blocking buffers and antigen/antibody diluents were chosen for further testing as they displayed similar SNR. Three detector antibody concentrations were then evaluated for each blocker/diluent combination, these were 0.05 µg/mL (used in the evaluation of blocking agents), 0.1 µg/mL and 0.2 µg/mL. In this screening, the chosen antigen diluent was 1% BSA in PBST for all samples determined from the previous evaluation of blocking buffers and diluents.

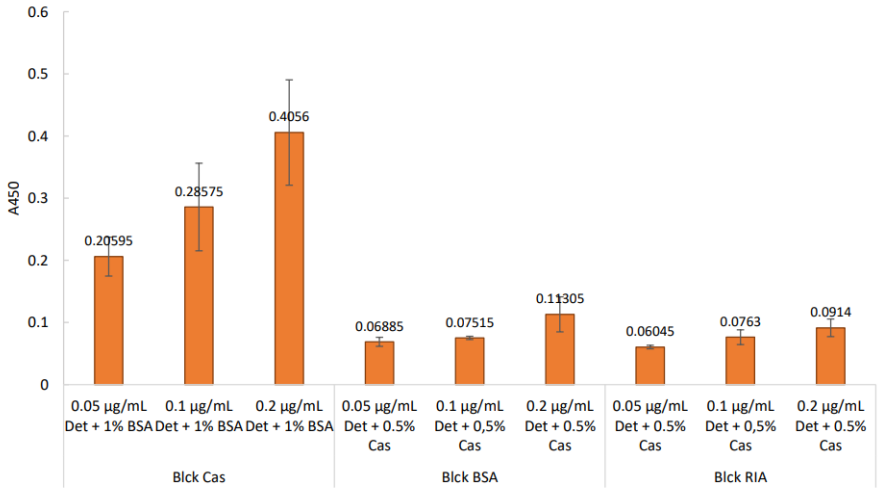


*Figure 16: Mean (n=2) absorbance (450 nm) background noise obtained during determination of detector antibody concentration.The RmAb158 capture antibody was applied in a 1 µg/mL concentration and the 3D6 5:5 OdT-detector antibody in concentrations of 0.05 - 0.2 µg/mL. Error bars represent the standard deviation.*

The obtained background noise for each detector antibody concentration are illustrated in Figure 16. It is evident that the detector antibody samples diluted in 1% BSA + PBST are very sensitive to changes in concentration and show variation between replicates, seen through the standard deviation. The high background noise consequently also cause a lower SNR for all detector antibody concentrations compared to the other two blocking buffer/diluent combinations. This combination will therefore not be used in the final protocol. The obtained background noise for the other combinations are however very similar which is expected as the only thing separating them is the blocking buffer. Both blocking buffers contain 1% BSA but the RIA buffer also has 2x higher NaCl concentration, 20x higher concentration of Tween 20 (1% vs 0.05%) and the addition of 1% SDS creating rougher conditions (see Supplementary Methods for complete reagent list). The SNR for each combination and concentration, seen in Figure 17, illustrated three good contenders for the final protocol (all using PBST + 1% BSA as antigen diluent) :
Block BSA + 0.1 µg/mL 3D6 5:5 in PBST +0.5% Casein
Block BSA + 0.2 µg/mL 3D6 5:5 in PBST +0.5% Casein
Block RIA + 0.2 µg/mL 3D6 5:5 in PBST +0.5% Casein

Because of the risk with of the RIA buffer stripping the plate of antibodies, the 2% BSA in PBST were chosen as the final blocking buffer along with a concentration of 0.1 µg/mL 3D6 5:5 detector antibody diluted in 0.5% Casein in PBST to keep the background noise low.

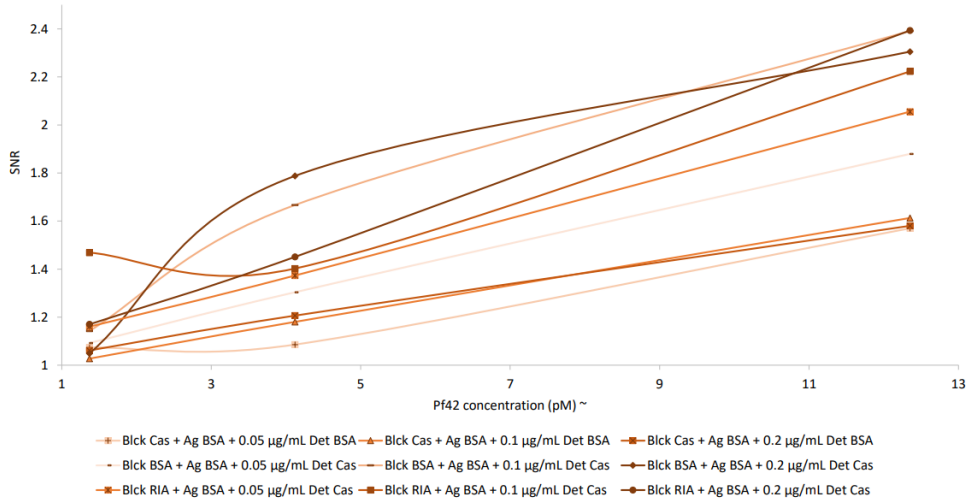


*Figure 17: SNR relative to the Pf42 concentration in pM obtained in the evaluation of detector antibody concentrations.*

### 4.3.4 Initial Estimation of Assay Precision

The results from the presented screenings contributed to the optimized final BOLD-amplified standard ELISA protocol. To make an initial estimation of the consistency and reliability in the protocol, three identical assays were run. Four control samples covering different points in the calibration curve were serially diluted 1:4 and run in triplicates for the BOLD-amplified assay and the standard assay. The applied concentrations were: 500 pM, 125 pM, 31,25 pM and 7.81 pM. These samples were numbered 1-4 and run together with duplicates of the calibration curve.

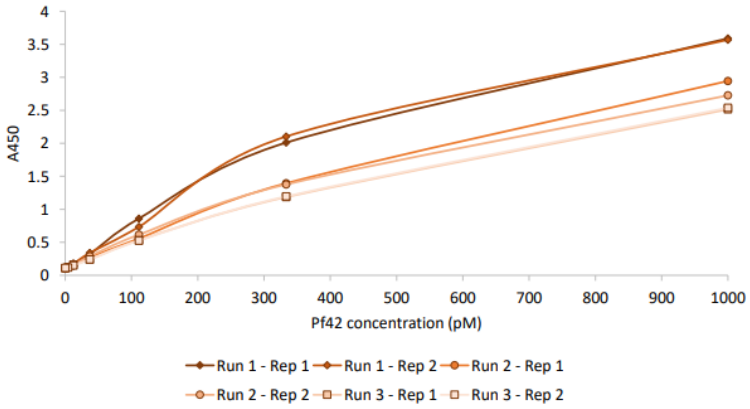


*(a) BOLD*

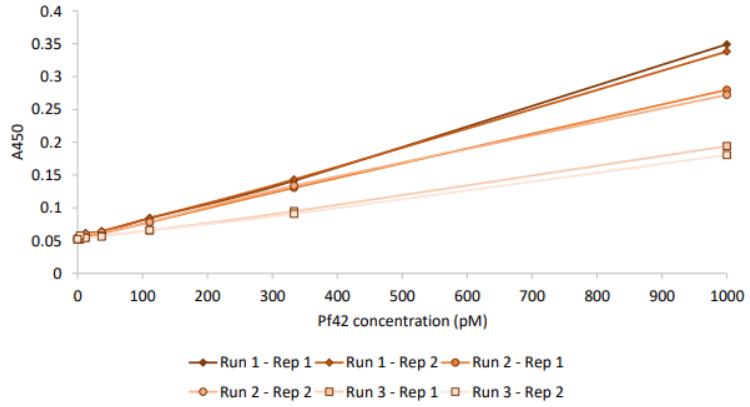


*(b) Standard*

*Figure 18: Calibration curves representing the obtained OD450 from each run, obtained during the initial estimation of assay precision. The RmAb158 capture antibody was applied in a 1 µg/mL concentration and the 3D6 5:5 OdT-detector antibody in a concentrations of 0.1 µg/mL. Samples were run in duplicates where Rep 1 and Rep 2 represents separate calibration curves within the run (Run 1, Run 2, Run 3).*

Replicates of the calibration curve from the three runs are displayed in Figure 18. The duplicate measurements show very good intra-assay precision, the inter-assay precision is however not good. There is a clear linear decrease in absorbance for the standard assay, similarities to this is also seen for the BOLD-amplified assay. However, there is a clear difference in the overall obtained OD-values compared to the standard assay. Concentrations of 1000 pM has a 10-fold higher value and for lower concentrations such as 4.12 pM, values obtained in the BOLD-assay are more than 2-fold. This stronger signal also contributes to values more easily distinguishable from the blank samples for lower antigen concentrations compared to the standard assay.

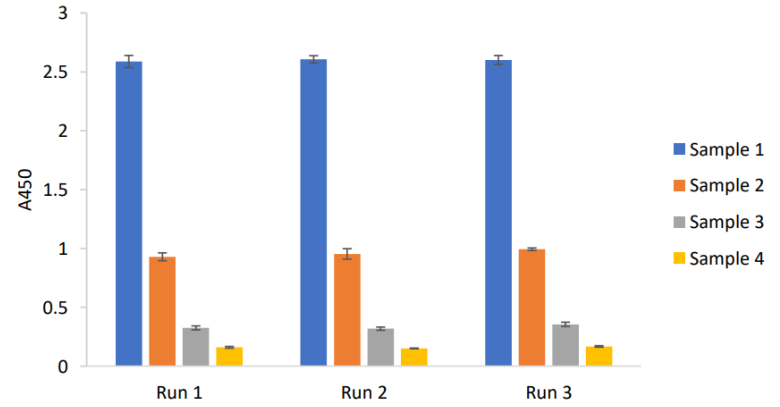


*(a) BOLD*

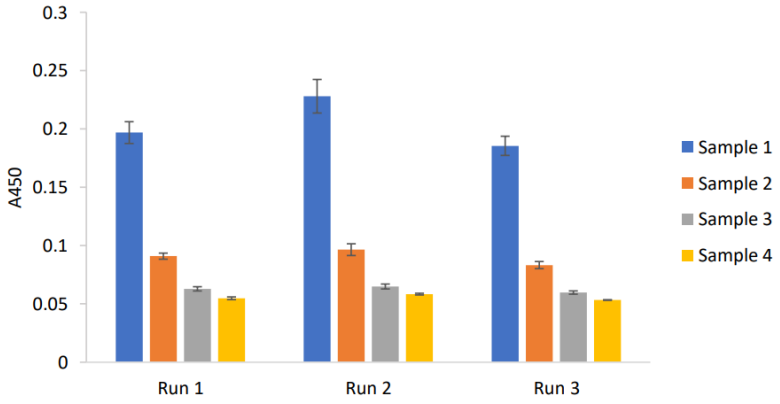


*(b) Standard*

*Figure 19: Obtained mean (n=3) absorbance (450 nm) for each control sample and their respective replicates (n=3) in each run. Error bars represent the standard deviation a) Control values from the BOLD-amplified assay b) Control values from the standard assay.*

The obtained mean absorbance values for each sample in the different runs are displayed in Figure 19. Values in the BOLD-amplified assay show high intra-assay precision and inter-assay precision seen through the standard deviation. Less precision overall is displayed in the standard assay. The precision is also confirmed through the CV (%) values presented in Tables 4 and 5 and where all intra-assay values are below 10% ranging from of 1.09%-5.17% for the BOLD-amplified assay and 0.43% - 6.32% for the standard assay across the different control samples. The inter-assay samples are below 15% for both assays ranging from from of 0.38%-6.25% for the BOLD-amplified assay and 9.12% - 11.11% for the standard assay

*Table 4: Intra-assay Coefficient of variation (%CV) for every control sample across the three runs.*

| | | Run 1 | | | Run 2 | | | Run 3 | | |
|---|---|---|---|---|---|---|---|---|---|---|
| Assay | Sample | Mean OD | SD OD | %CV | Mean OD | SD OD | %CV | Mean OD | SD OD | %CV |
| BOLD | 1 | 2.59 | 0.052 | 1.99 | 2.61 | 0.03 | 1.17 | 2.60 | 0.039 | 1.48 |
| | 2 | 0.93 | 0.033 | 3.60 | 0.95 | 0.044 | 4.64 | 0.99 | 0.011 | 1.09 |
| | 3 | 0.33 | 0.017 | 5.16 | 0.32 | 0.014 | 4.35 | 0.36 | 0.018 | 5.17 |
| | 4 | 0.16 | 0.008 | 4.92 | 0.15 | 0.003 | 1.82 | 0.17 | 0.006 | 3.75 |
| Standard | 1 | 0.20 | 0.009 | 4.75 | 0.23 | 0.014 | 6.32 | 0.19 | 0.008 | 4.43 |
| | 2 | 0.09 | 0.003 | 2.89 | 0.10 | 0.005 | 5.19 | 0.08 | 0.003 | 3.66 |
| | 3 | 0.06 | 0.002 | 2.92 | 0.07 | 0.002 | 3.24 | 0.06 | 0.001 | 2.37 |
| | 4 | 0.06 | 0.001 | 2.11 | 0.06 | 0.001 | 1.29 | 0.05 | 0.000 | 0.43 |

*Table 5: Inter-assay Coefficient of variation (CV(%)) for every control sample*

| Assay | Sample | Run 1 (mean OD) | Run 2 (mean OD) | Run 3 (mean OD) | Grand mean | SD | Inter-assay CV (%) |
|---|---|---|---|---|---|---|---|
| BOLD | 1 | 2.59 | 2.61 | 2.60 | 2.600 | 0.0100 | 0.38% |
| | 2 | 0.93 | 0.95 | 0.99 | 0.957 | 0.0306 | 3.19% |
| | 3 | 0.33 | 0.32 | 0.36 | 0.337 | 0.0208 | 6.18% |
| | 4 | 0.16 | 0.15 | 0.17 | 0.160 | 0.0100 | 6.25% |
| Standard | 1 | 0.20 | 0.23 | 0.19 | 0.207 | 0.0208 | 10.07% |
| | 2 | 0.09 | 0.10 | 0.08 | 0.090 | 0.0100 | 11.11% |
| | 3 | 0.06 | 0.07 | 0.06 | 0.063 | 0.0058 | 9.12% |
| | 4 | 0.06 | 0.06 | 0.05 | 0.057 | 0.0058 | 10.19% |

Through using the 4PL model and the obtained OD-values from the calibration curve, four parameters were generated describing the shape of the calibration curve. These parameters can be used to backcalculate the concentration values of LOD and LLOQ using the obtained OD-values for blank replicates. A total of 18 blank values were obtained for each assay resulting in a mean + SD of 0.1006 + 0.0067 for the BOLD-amplified assay, and 0.0561 + 0.0064 for the standard assay. The equation used for the calculation was the following: $x = C\times((A - D)/(y - D) - 1)^{(1/B)}$ with x being the concentration on pM and y being the OD LOD (mean + 2*SD) or OD LLOQ (mean + 10*SD). The calculated LOD and LLOQ values are displayed in Table 6.

*Table 6: Calculated values LOD and LLOQ for each run using the 4PL parameters for the calibration curve of each run. The LOD for run 1 was outside the curve range, illustrated with a dash.*

| | | LOD (OD) | LOD (pM) | LLOQ (OD) | LLOQ (pM) |
|---|---|---|---|---|---|
| BOLD | Run 1 | 0.114 | - | 0.168 | 11.6 |
| | Run 2 | 0.114 | 3.23 | 0.168 | 14.8 |
| | Run 3 | 0.114 | 3.17 | 0.168 | 16.1 |
| STD | Run 1 | 0.069 | 58.1 | 0.120 | 250 |
| | Run 2 | 0.069 | 70.4 | 0.120 | 284 |
| | Run 3 | 0.069 | 142 | 0.120 | 533 |

Based on calculations from the initial precision runs, the mean LOD and LLOQ for the BOLD-amplified assay is 3.2 pM and 14.2 pM respectively. For the standard assay, these values are 90.1 pM and 355 pM illustrating a valuable increase in sensitivity with the BOLD-amplified assay.

# 5 Discussion

The aim of this project was to develop and optimize a BOLD-amplified standard ELISA method for the detection of Aβ40 and Aβ42 with focus on detection of low concentrations in plasma. This entailed using Aβ-spiked samples in a simple matrix for improvement of the sensitivity in the standard ELISA assay while maintaining low background noise to ensure reliable detection in the early stages of Alzheimer's Disease.

## 5.1 Evaluation of Antibodies and Antigen for the BOLD-amplified Assay

Monoclonal antibodies 3D6 and RmAb158 has been evaluated both as capture antibodies and detector antibodies throughout several screenings. Both antibodies were successfully conjugated to oligo-dT primers using SPAAC, a crucial step for their function as detector antibodies in the BOLD-amplified assay. Conjugation was confirmed using μBCA and SDS-PAGE illustrating an increased number of observable bands for both ratios of DBCO ClickChem label and primer (5:5, 20:5) compared to the unconjugated antibody (Figure 7). The antibody with highest excess of label, the 20:5 ratio, illustrated the most prominent band shift which was as expected due to more available reactive groups for primer attachment. The SDS-PAGE also revealed that the samples were both heterogeneous with different degree of conjugation including non-conjugated chains. If these reduced chains are parts of a whole non-conjugated antibodies this could have affected the performance of the detector antibodies in the assay. If that would be the case, non-conjugated antibody could bind the antigen and outcompete the conjugated detector Ab. The measured signal would then misrepresent the true Aβ concentration in the sample as the non-conjugated antibodies does not produce any signal. However, no conclusions can be drawn from just this analysis as it uses reducing agents (DTT) in the samples. A non-reducing SDS-PAGE would have to be done do a more broad evaluation of the detector antibody sample content.

Biotinylation of 3D6 and RmAb158 was also performed to have a comparative standard assay for evaluation of the BOLD-amplified assay performance. A direct ELISA assay (Sup Tables 6 and 7) confirmed successful biotinylation and binding to the antigen through high signals when combined with a SA-HRP system for detection. However, no analysis of the degree of biotinylation was performed. Increasing biotinylation has been seen to cause loss of selectivity and affinity, weakening the interaction with its antigen. Perhaps through the biotin molecules causing a conformational change. There is also research suggesting that biotinylation might lead to interactions with unknown plasma proteins (Høyer-Hansen *et al.* 2000), something that should be considered not only in the standard ELISA but also in the BOLD-amplified ELISA, where the tertiary antibody is biotinylated. A possible solution to this is that the biotinylated antibodies can be used in combination with a StreptaClick® primer. The same detector antibody can then be used both for the BOLD and standard ELISA without the risk of unwanted interactions or conformational changes, making comparisons between the BOLD-amplified and standard assay less biased.

During screenings of the OdT-conjugated detector antibodies, it became evident that the conjugate with higher molar excess of DBCO (Click Chemistry label) relative primer, 20:5, displayed higher background noise than 5:5 without a significant increase in signal (Sup Figure 8). A higher excess of DBCO creates more available ground for binding free primer during the second step of the conjugation. More primer allows for an increased number of synthesized DNA/RNA stands which then also increases total number of bound tertiary antibodies to the detector antibody. It does not however increase the binding affinity to the antigen, thus underlying noise caused by the antibody may be emphasized in the BOLD-amplified assay without increasing signal. Additionally, with a higher excess of label there is a risk of steric hinderance and changes in the binding characteristics of the antibody (Vira *et al.* 2010).

High background noise was also an issue with 3D6 as a capture antibody (Sup Figure 9a). In the BOLD-amplified assay, very high absorbance values obtained even for samples without antigen. In the standard assay on the other hand, 3D6 gave concentration dependent values and low background noise. These issues were not seen with the RmAb158 antibody when used for capture, suggesting that the 3D6 antibody has some underlying issues. One hypothesis is that it binds very strongly to the plate and that the washing step post overnight incubation and blocking buffers used to prevent non-specific binding is not sufficient enough. Perhaps this issue could be solved using a stronger blocking buffer, but this was not investigated further due to time constraints.

Further, one limitation of this study is that the immobilization of the capture antibody to the plate was not a fully controlled process. The immobilization of the antibody plays a crucial role in the sensitivity and the limit of detection of the assay. The orientation

of which the antibody binds to the plate could affect its performance and the assay sensitivity overall if the antigen binding site is partially or fully blocked. Non-uniform distribution of the antibody on the plate also affects the detection (Wang *et al.* 2019). Increasing binding to the plate with the proper orientation, perhaps with focus on immobilization of the Fc region, through other methods than physical absorption could then possibly improve the detection limit.

During the development of the final assay two types of Aβ structures were tested, the monomeric Aβ40 and the protofibrillar Aβ42. Pf42 showed higher signals for the lower concentration ranges while the monomeric Aβ40 required the application of higher concentrations on the assay for detection in the BOLD-amplified and standard assay. This is likely due to the binding specificity of 3D6 and RmAb158 where 3D6 binds AA 1-5 on the N-terminal of monomers and aggregates and RmAb158 binds AA 3-8 on only protofibrils (allegedly). Since these two antibodies share similar binding sites, this could affect the ability of both antibodies binding the Aβ40 monomers simultaneously, something that is likely not a problem for the protofibrils since the structures are larger and more complex. This offers more available binding sites for the 3D6 and RmAb158 antibodies.

## 5.2 Shortened Incubation Time for Reduced Background Noise

The starting BOLD-amplified assay protocol consisted of a 3-day protocol with two overnight incubations and several longer incubations in between these. One hypothesis was that shorter incubation times would reduce the amount of non-specific binding resulting in lower background noise (signal originating from a well without Pf42 antigen). Decreasing the overall incubation time of the protocol would also make the workflow of the assay more effective. Although the decrease of the capture antibody incubation time resulted in lowered background noise, it also resulted in a loss of Pf42-specific signal, likely due to insufficient immobilization of antibody to the plate. Shortening the incubation time for the detector antibody and SA-HRP did also result in Pf42-specific signal loss, however it also reduced the background noise by almost half (Figure 10).

Although the SNR was not improved significantly, the overnight capture antibody incubation period was kept and the detector antibody and SA-HRP incubation periods were shortened from 180 min + 60 min to 60 min + 30 min as this lowered the background noise substantially from 0.58 OD to 0.29 OD while also shortening the overall protocol by 2,5 hours.

During the screening of incubation times for the capture and detector antibodies, one

assay per detector antibody were run. The obtained OD450 values revealed that the RmAb158 capture antibody - 3D6 detector antibody assay generated better signals and better concentration dependence at lower Pf42 concentrations than the RmAb158 capture antibody - RmAb158 detector antibody assay. Although the antibodies have overlapping binding sites, this overlap likely allows for more available binding sites compared to using the same type of capture and detector antibody.

Another hypothesis related to incubation time was that the Aβ may aggregate further during the overnight incubation as signal was seen with the Aβ40 monomer in the RmAb158 capture antibody assay. Aβ40 and Aβ42 are known to aggregate rapidly over time with experiments suggesting that this also occur during the ELISA incubation process. There are also speculations suggesting that a longer incubation may result in formation of larger aggregates or protofibrils. (Metzendorf *et al.* 2025). To prevent this, two shorter antigen incubation times, using Pf42 antigen, were tested against the overnight incubation. Results illustrated too much loss in signal to make any adjustments in the optimized protocol. The Aβ likely requires a longer incubation time for proper binding to the plate.

## 5.3 Successful Combination of Blocking Agents

Although lowering the background noise was possible to some degree through the evaluation and selection of certain capture/detector antibody combinations and the reduction of incubation time, blocking unoccupied binding sites is essential for reducing non-specific binding. However, there are some research suggesting that certain detection systems and antibodies can cross-react with certain proteins such as BSA causing inaccurate results and affecting the performance of the assay (Jiang *et al.* 2021). It is therefore important to test different blocking buffers to the different components.

The screening involved 18 different combinations of blocking buffer, antigen diluent and detector antibody diluent where certain combinations were not ideal for this system. BSA in PBST as a detector diluent gave very high background noise for all combinations, possibly due to interference with the SA-HRP system where the streptavadin might not only bind the biotin on the tertiary antibody but also bind biotin molecules present at blocked binding sites and thus give false positive signals. The opposite results were seen with RIA buffer as a detector diluent. While the measurements displayed very low background noise, the Pf42-specific signals were also low suggesting that the detergents in the buffer prevented binding of the detector to the plate, possibly through denaturation of the antibody or in other ways disrupting the antigen-antibody binding. Detergents such as Tween20 has been reported to reduce non-specific binding by preventing non-specific hydrophobic interactions however, it has also been reported to cause protein

desorption, increase background noise and reduce the sensitivity of an ELISA. Other detergents such as SDS, and Triton is typically also not recommended in blocking buffers as they could break the antigen-antibody interaction as well as inhibit the substrate-enzyme interaction (Jiang *et al.* 2021). They should therefore be used with caution.

Besides blocking buffers, washing in between each incubation step is essential for the removal of unbound components. This is done to ensure that non-specific binding is minimal and that the assay maintains its specificity (Jeon *et al.* 2025). The washing steps in starting protocol involves a 3x wash in between each incubation period. As the background noise was still high, the washing steps were increased to a 8x wash in between every incubation step. The 3x wash post blocking of the capture antibody was kept to ensure that the of blocking unbound sites on the plate was not disrupted. Comparing the background from the incubation time screening and the background noise in the blocker screening where Casein was used in all 3 steps the OD450 values are 0.29 vs 0.094. This reduction in noise is likely not only due to the increased number of washing steps but also the higher concentration of Casein in the PBST (0.5% vs 0.1% Casein).

## 5.4 Incresed SNR with Higher Detector Antibody Concentration

As several combinations showed good SNR with low background noise at low antigen concentrations, these were tested with higher detector antibody concentrations to asses their performance better. Although the BSA in the detector diluent gave very high background noise, one combination also had a relatively good SNR. However, the increase in detector antibody concentration illustrated that the background noise under these conditions were very sensitive to changes and thus not appropriate for the final optimized protocol. It is possible that the detector antibody does cross-react with BSA due to the large increase in noise that is not seen with Casein in the detector antibody diluent.

Regarding the blocking buffers 2% BSA in PBS and RIA buffer, both showed similar results which was as expected as the blocking agent in the RIA buffer is 1% BSA. The combination with BSA in the blocking buffer show slightly better SNR while also containing no detergents compared to the RIA buffer. As previously mentioned, there is a risk when using detergents at too high concentrations when in solutions with biological reagents as it could affect their functionality. While BSA is a commonly used blocker, besides the risk or cross-reactivity, it has also been reported to easily be washed away with PBST due to weak binding to the plate (Jiang *et al.* 2021). So while it might work well in these particular conditions, it does not guarantee good assay performance in other settings. Taking this into consideration, the combination of using 2% in PBS as block-

ing buffer, 1% BSA in PBST as antigen diluent and 0.1 µg/mL of 3D6 OdT-detector antibody in 0.5% Casein in PBST was therefore presents the best choice for this system.

## 5.5 Initial Estimation of Assay Precision

To make an initial estimation of the precision in the assay protocol, an assay containing a calibration curve and control samples was run three times with identical conditions and reagents lots during the span of 2 weeks. The control samples were serially diluted and frozen in aliqotes, two per sample, thawed and used only once. These samples performed very similarly in reference to the obtained absolute absorbance of the BOLD-amplified assay, indicating that the Exazym® reagents are consistent and working. However, different lots of the reagents should be tested in the same conditions to make a more reliable and elaborate evaluation of the performance. Obtained absorbance values from the standard assay had some more variation, suggesting there might be some variation in other reagents such as the diluents which were made fresh each run. Signal could also be affected by the placement of standard-assay wells in 4°C post wash during the Exazym® steps. It should also be noted that the same incubation conditions were used for both assays in this estimation, the ideal conditions might be different for the standard ELISA therefore affecting the results.

The obtained absorbance values of the calibration curves of each run illustrates a linear decrease across the different runs, the last being around 1 OD unit lower for 1000 pM in the BOLD-amplified assay. A limitation of this evaluation was that the same Pf42 sample was used each run, going through freeze-thaw cycles that likely affected the sample quality and therefore resulted in large differences in-between assays. It is possible that some of the aggregates precipitated or degraded during these freeze-thaw cycles causing a decrease in captured antigen on the plate. This hypothesis arises from the comparison to the control samples, where the same reagents and conditions were used except no freeze-thaw cycles were performed. Considering only intra-assay precision, the obtained OD-values seen in Figure 9, were very similar across all runs again pointing to issues with the antigen sample handling. In future testing, the antigen samples should only be used once for the calibration curve similarly to the control samples.

Since the 4PL model is adjusted to the obtained calibration curve, this resulted in differences in the calculated parameters between the different runs. This further affected the estimation of the LOD and LLOQ for the BOLD-amplified assay and the standard assay. For a more accurate estimation, these parameters should be based on consistent OD-values across several more runs to give a reliable representation of the calibration curve, resulting in a more accurate representation of the assay sensitivity.

Taking these points into consideration, the obtained values from control samples of the two comparative assays (see Figure 10) are more easily distinguishable from the background in the BOLD-amplified assay. Signals are also 10-fold higher for the high and higher middle concentration range and (500 pM, 125 pM) and around 5-fold higher for the lower middle range and lower range (31.3 pM, 7.81 pM). These results collectively and strongly illustrates that the BOLD-amplified ELISA effectively detects and quantifies Pf42.

## 5.6 Relevance

There are several immunoassay platforms that have demonstrated ultrasensitive detection of Aβ biomarkers at levels that traditional ELISAs fail to detect. The SIMOA technology that is a digital ELISA platform, enables quantification of a wide range of biomarkers in a large range of concentrations including plasma Aβ ratios (Sahrai *et al.* 2023). The Amyblood immunoassay for example, that is used on the SIMOA platform, has LLOQs at 1.6 pg/mL for Aβ42 and 1.6 pg/mL for Aβ40. Another immunoassay, the Quanterix tiplex assay has LLOQs of are 0.34 pg/mL and 0.16 pg/mL respectively. (Thijssen *et al.* 2021). Further, electrochemiluminescence immunoassays (ECLIA) are increasingly becoming more popular due to its increased sensitivity compared to the conventional ELISA. The sensitivity is in the femtomolar range while also being less susceptible to cross-reactivity with different reagents (Khan *et al.* 2025).

In this project, no estimation of the true LOD and LLOQ in pg/mL could be done as the size of the Pf42 stuctures in the sample is unknown. However, based on the initial calculations of the LLOQ for the BOLD-amplified assay and assuming that the smallest protofibrils could be 100 kDa (Ono & Tsuji 2020), this would result in a minimum LLOQ of 1.42 pg/mL being in similar ranges as currently available platforms. Considering that this solution does not need any expensive equipment or instruments, only standard ELISA equipment already available in most labs, this assay presents great potential.

# 6 Future research

There are many parameters and conditions to investigate in future research, the examples mentioned here are only a few. This creates a great opportunity in exploring all different kinds of directions.

Future optimization and fine tuning of this assay could focus on the introduction of biological samples with varying matrices. Optimization of the assay-parameters in this project has been adjusted based on its performance with Aβ-spiked samples in a simple matrix. Protein samples with more complex matrices such as plasma might behave differently in the selected conditions. Because of the additional biological components in the matrix that might interfere with system, the assay likely requires adjustments based on factors such as the type of matrix, the species of the sample etc to reduce background noise caused by these components. These adjustments might for example involve optimization of buffer components or incubation conditions.

Other potential directions could involve testing of alternative capture and detector antibody candidates. The antibodies utilized this project have very similar binding sites which could sterically hinder the antigen-antibody binding to some degree, especially if they are monomers. The sensitivity if the assay might therefore be increased if using capture and detector antibodies with for example one binding site in the N-terminal and the other in the C-terminal of the antigen. In addition to this, other conjugation ratios and strategies of the detector antibody might optimize the binding conditions. These directions are not only relevant for the optimization of the Pf42 assay but for also for further evaluation of the monomeric Aβ assay and its potential in being used together with BOLD.

Further related to the conjugation of the OdT-detector antibodies, introducing purification of the detector antibody post conjugation with primer might decrease the background. As primer is added in excess to the Click Chemistry labeled detector antibody in the last step of the conjugation, free primer is still present in the final sample. This can lead to non-specific hybridization and possible contribution to background noise.

# 7 Conclusion

This project has highlighted the potential of applying signal amplification methods such as BOLD on standard ELISA formats for efficient detection and quantification of biomarkers related to Alzheimer's disease. The project has illustrated the importance of balancing signal and background noise for a reliable and sensitive assay. Throughout the evaluations of different parameters, the assay has displayed great performance without any special equipment, increasing the sensitivity of an already working standard immunoassay. Maintaining high sensitivity without expensive instruments and complex protocols, highlights a big advantage of using BOLD compared to other platforms

such as SIMOA that does not have the same flexibility. Although this assay has been optimized to some degree, evaluations of the precision has shown that continued optimization is needed for the advancement of this assay into a research and diagnostic tool. The continued research and optimization of this assay should especially focus on incorporating Aβ samples with more complex matrices for a more comprehensive estimation of its performance.

# Ethical Considerations

The broader aim of this project was to improve the sensitivity of an already existing diagnostic tool for the detection of biomarkers associated with Alzheimer's disease. AD affects millions of people worldwide. Despite decades of advances in research and advances, there are still many unresolved questions regarding the pathology and the pathophysiology. This makes the disease one of the most relevant research areas in neuroscience with the detection of biomarkers being central to diagnosis and understanding of the mechanisms. For biomarkers such as Aβ and pTau, many of the reliable detection methods for diagnostics are dependable on CSF sample collection, an invasive procedure for the patient, and expensive imaging instruments. In addition to the low biomarker concentrations in early stages of the disease, diagnosis at the primary care level becomes very difficult.

One emerging solution to this problem is using blood samples in immunoassays such as ELISA. However, levels of Aβ are lower in blood than in the CSF, requiring an ultra-sensitive method for detection. The BOLD-technology is able to meet this criteria through its signal amplification properties being applicable to a standard sandwich ELISA. It has already shown great results in the detection of pTau 181 significantly lowering the limit of detection and this project further illustrates its potential in improving the sensitivity in detection of Aβ.

If optimized, the assay has exceeding benefits, not only on the societal and economical level but also on the individual level. Compared to many other diagnostic tools that require expensive instruments, the BOLD-amplified ELISA is fast, inexpensive and accessible. As this can be done without any complex equipment, it creates opportunities for places where such infrastructure is limited to test and detect signs of the disease earlier. This refers not only to smaller labs but also to low- and middle-income countries where healthcare professionals have limited economical means. Responsibilities

currently placed on larger healthcare facilities could thus be redistributed and more balanced.

Historically, AD has only been possible to detect in the later stages of the disease. An early detection creates a window that allows for treatments or enrollments in clinical trials to be introduced earlier, possibly before any major symptoms are visible. Delaying hospitalization and long-term care special facilities would reduce the overall burden on healthcare systems and leave room for treatment of other diseases.

On an individual level, early diagnosis would significantly increase the quality of life, not only for the patient, but also for their loved ones. It allows the individual to plan ahead for their future. While still having cognitive capacity they can make informed decisions about their finances, long-term care arrangements and express any wishes regarding their passing. It also provides the opportunity to make lifestyle changes such as dietary changes, increase exercise or cognitive engagement for additional prevention. Lastly, an early diagnosis enables families to seek support in social networks or through counseling, preventing uncertainties and anxiety about the future.

# AI Statement

AI tools has been employed during the writing of this thesis to assist with grammar correction and sentence refinement. AI has also been used to generate code for the 4PL model used in the μBCA analysis and the precision analysis. These tools has only been used as supportive aids in accordance to anti-plagiarism standards to ensure academic integrity and have not contributed to the original content of the thesis. All ideas, interpretations, analyses and discussion is solely attributed to the author.

# Acknowledgements

First and foremost, I would like to express gratitude to my supervisor Dr. Peter Stenlund for giving me the opportunity to work on this project. I would like to thank him for the invaluable support and guidance throughout these past months. The insightful discussions and feedback has been trivial for the progress of the project and the completion of this thesis.

I would also like to thank Bence Réthi for taking time to review and discuss the results, showing enthusiasm and support in the development of the project. Further, I would like to give a huge thanks to the entire team at Cavidi for creating such a positive working environment that invites collaboration and asking questions. It has truly made this experience much more enjoyable. My sincerest thanks to my subject reader Ylva Ivarsson for her advice and feedback, especially during the finalization of this thesis.

Lastly, I would like to thank Lena Henriksson for being there for us students, always available to answer questions and offer to help. Your support is very much appreciated!

# References

Alawode DOT, Fox NC, Zetterberg H, Heslegrave AJ. 2022. Alzheimer's Disease Biomarkers Revisited From the Amyloid Cascade Hypothesis Standpoint. Frontiers in Neuroscience 16: 837390.

Alhajj M, Zubair M, Farhana A. 2025. Enzyme Linked Immunosorbent Assay. StatPearls, StatPearls Publishing, Treasure Island (FL).

Anthropic. 2026. Reproducerbarhet för ELISA-analys.

Armbruster DA, Pry T. 2008. Limit of Blank, Limit of Detection and Limit of Quantitation. The Clinical Biochemist Reviews 29: S49–S52.

Arya SK, Estrela P. 2018. Recent Advances in Enhancement Strategies for Electrochemical ELISA-Based Immunoassays for Cancer Biomarker Detection. Sensors 18.

Aydin S, Emre E, Ugur K, Aydin MA, Sahin □, Cinar V, Akbulut T. 2025. An overview of ELISA: a review and update on best laboratory practices for quantifying peptides and proteins in biological fluids. The Journal of International Medical Research 53: 03000605251315913.

Azargoonjahromi A. 2024. The duality of amyloid-β: its role in normal and Alzheimer's disease states. Molecular Brain 17: 44.

Baek S, Lee JC, Byun BH, Park SY, Ha JH, Lee KC, Yang SH, Lee JS, Hong S, Han G, Lim SM, Kim Y, Kim HY. 2025. Combination of Aβ40, Aβ42, and Tau Plasma Levels to Distinguish Amyloid-PET Positive Alzheimer Patients from Normal Controls. Experimental Neurobiology 34: 1–8.

Bhat R, Crowe EP, Bitto A, Moh M, Katsetos CD, Garcia FU, Johnson FB, Trojanowski JQ, Sell C, Torres C. 2012. Astrocyte Senescence as a Component of Alzheimer's Disease. PLoS ONE 7: e45069.

Bouwman FH, Frisoni GB, Johnson SC, Chen X, Engelborghs S, Ikeuchi T, Paquet C, Ritchie C, Bozeat S, Quevenco F, Teunissen C. 2022. Clinical application of CSF biomarkers for Alzheimer's disease: From rationale to ratios. Alzheimer's & Dementia : Diagnosis, Assessment & Disease Monitoring 14: e12314.

del Campo M, Jongbloed W, Twaalfhoven HAM, Veerhuis R, Blankenstein MA, Teunissen CE. 2015. Facilitating the Validation of Novel Protein Biomarkers for Dementia: An Optimal Workflow for the Development of Sandwich Immunoassays. Frontiers in Neurology 6.

Cavacini L, Greenspan N. 2013. Immunoglobulin function. Clinical Immunology, Elsevier, 183–192.

Cavidi. 2024. Application of BOLD Technology in Assessing Biomarkers Within Neuroscience. Technical report.

Cavidi. 2025. Efficient Oligo-dT Primer Conjugation for BOLD Amplified ELISA.

Charles A Janeway J, Travers P, Walport M, Shlomchik MJ. 2001. The structure of a typical antibody molecule. Immunobiology: The Immune System in Health and Disease. 5th edition, Garland Science.

Chen Gf, Xu Th, Yan Y, Zhou Yr, Jiang Y, Melcher K, Xu HE. 2017. Amyloid beta: structure, biology and structure-based therapeutic development.

Chiu ML, Goulet DR, Teplyakov A, Gilliland GL. 2019. Antibody Structure and Function: The Basis for Engineering Therapeutics. Antibodies 8: 55.

Debets MF, van Berkel SS, Dommerholt J, Dirks ATJ, Rutjes FPJT, van Delft FL. 2011. Bioconjugation with Strained Alkenes and Alkynes. Accounts of Chemical Research 44: 805–815.

Dyck CHv, Swanson CJ, Aisen P, Bateman RJ, Chen C, Gee M, Kanekiyo M, Li D, Reyderman L, Cohen S, Froelich L, Katayama S, Sabbagh M, Vellas B, Watson D, Dhadda S, Irizarry M, Kramer LD, Iwatsubo T. 2023. Lecanemab in Early Alzheimer's Disease. New England Journal of Medicine 388: 9–21. _eprint: https://www.nejm.org/doi/pdf/10.1056/NEJMoa2212948.

Elamin SA, Al Shibli AN, Shaito A, Al-Maadhadi MJMB, Zolezzi M, Pedersen S. 2025. Anti-amyloid monoclonal antibody therapies in Alzheimer's disease – a scoping review. Neuroscience 589: 50–61.

Engvall E, Perlmann P. 1971. Enzyme-linked immunosorbent assay (ELISA). Quantitative assay of immunoglobulin G. Immunochemistry 8: 871–874.

Fandos N, Pérez-Grijalba V, Pesini P, Olmos S, Bossa M, Villemagne VL, Doecke J, Fowler C, Masters CL, Sarasa M. 2017. Plasma amyloid β 42/40 ratios as biomarkers for amyloid β cerebral deposition in cognitively normal individuals. Alzheimer's & Dementia : Diagnosis, Assessment & Disease Monitoring 8: 179–187.

Feldcamp A, Carey J. 1996. IMMUNE FUNCTION AND ANTIBODY STRUCTURE. Immunoassay, Academic Press, 5–24.

Gibbs J. 2012. Selecting the Detection System - Colorimetric, Fluorescent, Luminescent Methods - - ELISA Technical Bulletin - No. 5 .

Greenspan NS. 2023. Epitopes, paratopes, and other topes 30 years on: Understanding what we are talking about. Human Immunology 84: 429–438.

Gu L, Guo Z. 2013. Alzheimer's Aβ42 and Aβ40 peptides form interlaced amyloid fibrils. Journal of neurochemistry 126: 305–311.

Gunes S, Aizawa Y, Sugashi T, Sugimoto M, Rodrigues PP. 2022. Biomarkers for Alzheimer's Disease in the Current State: A Narrative Review. International Journal of Molecular Sciences 23: 4962.

Harrand R. 2023. ELISA Analysis in Python.

Hein CD, Liu XM, Wang D. 2008. Click Chemistry, a Powerful Tool for Pharmaceutical Sciences. Pharmaceutical research 25: 2216–2230.

Hu R, Sou K, Takeoka S. 2020. A rapid and highly sensitive biomarker detection platform based on a temperature-responsive liposome-linked immunosorbent assay. Scientific Reports 10: 18086.

Høyer-Hansen G, Hamers MJAG, Pedersen AN, Nielsen HJ, Brünner N, Danø K, Stephens RW. 2000. Loss of ELISA specificity due to biotinylation of monoclonal antibodies. Journal of Immunological Methods 235: 91–99.

Ivell R, Teerds K, Hoffman GE. 2014. Proper Application of Antibodies for Immunohistochemical Detection: Antibody Crimes and How to Prevent Them. Endocrinology 155: 676–687.

Jeon HB, Song DY, Park YJ, Kim DM. 2025. Enhancing ELISA Sensitivity: From Surface Engineering to Synthetic Biology. Biosensors 15: 434.

Jiang X, Wu M, Albo J, Rao Q. 2021. Non-Specific Binding and Cross-Reaction of ELISA: A Case Study of Porcine Hemoglobin Detection. Foods 10: 1708.

Johansson L, Sandberg A, Nyström S, Hammarström P, Hallbeck M. 2024. Amyloid beta 1-40 and 1-42 fibril ratios and maturation level cause conformational differences with minimal impact on autophagy and cytotoxicity. Journal of Neurochemistry 168: 3308–3322. _eprint: https://onlinelibrary.wiley.com/doi/pdf/10.1111/jnc.16201.

Kapoor M, Heston TF, Kasi A. 2025. PET Scanning. StatPearls, StatPearls Publishing, Treasure Island (FL).

Kempermann G, Song H, Gage FH. 2015. Neurogenesis in the Adult Hippocampus. Cold Spring Harbor Perspectives in Biology 7: a018812.

Khan RMN, Zeng Y, Lanihun AA, Arisa OT, Horner JL, Figg WD. 2025. Recent Advances in Bioanalytical Methods for Quantification and Pharmacokinetic Analyses of Antibody–Drug Conjugates. The AAPS journal 27: 138.

Kumar A, Sidhu J, Lui F, Tsao JW. 2025. Alzheimer Disease. StatPearls, StatPearls Publishing, Treasure Island (FL).

Lang L, Clifford A, Wei L, Zhang D, Leung D, Augustine G, Danat IM, Zhou W, Copeland JR, Anstey KJ, Chen R. 2017. Prevalence and determinants of undetected dementia in the community: a systematic literature review and a meta-analysis. BMJ Open 7: e011146.

Lipman NS, Jackson LR, Trudel LJ, Weis-Garcia F. 2005. Monoclonal Versus Polyclonal Antibodies: Distinguishing Characteristics, Applications, and Information Resources. ILAR Journal 46: 258–268.

MacLeod R, Hillert EK, Cameron RT, Baillie GS. 2015. The role and therapeutic targeting of α-, β- and γ-secretase in Alzheimer's disease. Future Science OA 1: FSO11.

Margetis K, Baker S. 2025. Physiology, Cerebral Spinal Fluid. StatPearls [Internet], StatPearls Publishing.

Mehta PD, Patrick BA, Miller DL, Coyle PK, Wisniewski T. 2020. A Sensitive and Cost-Effective Chemiluminescence ELISA for Measurement of Amyloid-β 1-42 Peptide in Human Plasma. Journal of Alzheimer's disease : JAD 78: 1237–1244.

Metzendorf NG, Sehlin D, Hultqvist G. 2025. Key considerations for ELISA-based quantification of diverse amyloid beta forms in murine brain homogenates. Frontiers in Neuroscience 19.

Ono K, Tsuji M. 2020. Protofibrils of Amyloid-β are Important Targets of a Disease-Modifying Approach for Alzheimer's Disease. International Journal of Molecular Sciences 21: 952.

OpenAI. 2025. 4PL analys. Version 5.2.

OpenAI. 2026. 4PL ELISA ChatGPT.

O'Brien RJ, Wong PC. 2011. Amyloid Precursor Protein Processing and Alzheimer's Disease. Annual review of neuroscience 34: 185–204.

Pallarés-Moratalla C, Bergers G. 2024. The ins and outs of microglial cells in brain health and disease. Frontiers in Immunology 15: 1305087.

Peng HP, Lee KH, Jian JW, Yang AS. 2014. Origins of specificity and affinity in antibody–protein interactions. Proceedings of the National Academy of Sciences 111: E2656–E2665.

Peng Q, Zhang Z. 2021. The fluid biomarkers of Alzheimer's disease. Brain Science Advances 7: 1–16.

Piaceri I, Nacmias B, Sorbi S, Piaceri I, Nacmias B, Sorbi S. 2013. Genetics of familial and sporadic Alzheimer's disease. Frontiers in Bioscience-Elite 5: 167–177.

Porsteinsson AP, Isaacson RS, Knox S, Sabbagh MN, Rubino I. 2021. Diagnosis of Early Alzheimer's Disease: Clinical Practice in 2021. The Journal of Prevention of Alzheimer's Disease 8: 371–386.

Rojas G. 2022. Understanding and Modulating Antibody Fine Specificity: Lessons from Combinatorial Biology. Antibodies 11.

Sahrai H, Norouzi A, Hamzehzadeh S, Majdi A, Kahfi-Ghaneh R, Sadigh-Eteghad S. 2023. SIMOA-based analysis of plasma NFL levels in MCI and AD patients: a systematic review and meta-analysis. BMC Neurology 23: 331.

Schultheiss OC, Stanton SJ. 2009. Assessment of Salivary Hormones. Methods in Social Neuroscience .

Schöll M, Verberk IMW, Campo Md, Delaby C, Therriault J, Chong JR, Palmqvist S, Alcolea D. 2024. Challenges in the practical implementation of blood biomarkers for Alzheimer's disease. The Lancet Healthy Longevity 5.

Siddiqui MZ. 2010. Monoclonal Antibodies as Diagnostics; an Appraisal. Indian Journal of Pharmaceutical Sciences 72: 12–17.

Stapleton S, Kennedy RO, Tully E. 2005. IMMUNOASSAYS | Production of Antibodies. Worsfold P, Townshend A, Poole C, editors, Encyclopedia of Analytical Science (Second Edition), Elsevier, Oxford, 306–316. Second edition edition.

Thijssen EH, Verberk IMW, Vanbrabant J, Koelewijn A, Heijst H, Scheltens P, van der Flier W, Vanderstichele H, Stoops E, Teunissen CE. 2021. Highly specific and ultrasensitive plasma test detects Abeta(1–42) and Abeta(1–40) in Alzheimer's disease. Scientific Reports 11: 9736.

Tiwari S, Atluri V, Kaushik A, Yndart A, Nair M. 2019. Alzheimer's disease: pathogenesis, diagnostics, and therapeutics. International Journal of Nanomedicine 14: 5541–5554.

Van Regenmortel MHV. 2014. Specificity, polyspecificity, and heterospecificity of antibody-antigen recognition. Journal of Molecular Recognition 27: 627–639. _eprint: https://onlinelibrary.wiley.com/doi/pdf/10.1002/jmr.2394.

Van Weemen BK, Schuurs AHWM. 1971. Immunoassay using antigen-enzyme conjugates. FEBS letters 15: 232–236.

Vidyakina A, Silonov S, Govdi A, Ivanov A, Podolskaya E, Balova I, Bräse S, Danilkina N. 2024. Key role of cycloalkyne nature in alkyne-dye reagents for enhanced specificity of intracellular imaging by bioorthogonal bioconjugation. Organic & Biomolecular Chemistry 22: 7637–7642.

Vira S, Mekhedov E, Humphrey G, Blank PS. 2010. Fluorescent labeled antibodies - balancing functionality and degree of labeling. Analytical biochemistry 402: 146–150.

Viswanathan R, Carroll M, Roffe A, Fajardo JE, Fiser A. 2024. Computational prediction of multiple antigen epitopes. Bioinformatics 40: btae556.

Wang C, Lakshmipriya T, Gopinath SCB. 2019. Amine-Aldehyde Chemical Conjugation on a Potassium Hydroxide-Treated Polystyrene ELISA Surface for Nanosensing an HIV-p24 Antigen. Nanoscale Research Letters 14: 21.

Wang S, Mims PN, Roman RJ, Fan F. 2016. Is Beta-Amyloid Accumulation a Cause or Consequence of Alzheimer's Disease? Journal of Alzheimer's parkinsonism & dementia 1: 007.

WHO. 2017. Global action plan on the public health response to dementia 2017–2025. Global action plan, World Health Organization, Geneva.

WHO. 2025. Dementia.

Yalow RS, Berson SA. 1960. IMMUNOASSAY OF ENDOGENOUS PLASMA INSULIN IN MAN. Journal of Clinical Investigation 39: 1157–1175.

Zarovniaeva V, Anwar S, Kazmi S, Cortez Perez K, Sandhu S, Mohammed L. 2025. The Role of PET Detection of Biomarkers in Early Diagnosis, Progression, and Prognosis of Alzheimer's Disease: A Systematic Review. Cureus 17: e77781.

Zeliger H. 2023. Chapter 13 - Alzheimer's disease. Oxidative Stress - Its Mechanisms and Impacts on Human Health and Disease Onset, Elsevier Inc, USA, 291–297.

Zubair M, Singh C, Farhana A. 2026. Enzyme-Linked Immunosorbent Assay (ELISA). StatPearls, StatPearls Publishing, Treasure Island (FL).

# A Supplementary Tables

### A.0.1 Conjugation of Antibodies

*Sup Table 1: Final volumes added for each component and reagent used in the conjugation of the antibodies 3D6 and RmAb158.*

| Molar ratio of Oligo-dT primer and ClickChem label | Volume (µL) DBCO ClickChem Label | Volume (µL) of antibody | Volume (µL) of Quenching Buffer | Volume (µL) of PBST to reach final vol of 80 µL | Volume (µL) of Azide oligo-dT primer |
|---|---|---|---|---|---|
| 3D6 5:5 | 2.7 | 40.0 | 6 | 31.3 | 6.5 |
| 3D6 20:5 | 10.9 | 40.0 | 6 | 23.1 | 6.5 |
| RmAb158 5:5 | 2.7 | 40.0 | 6 | 31.3 | 6.5 |
| RmAb158 20:5 | 10.9 | 40.0 | 6 | 23.1 | 6.5 |

*Sup Table 2: Dilution scheme for Bovine Gamma Globulin (BGG) protein standards used in µBCA.*

| Vial | Stock conc (µg/mL) | Vol stock(µL) | Vol PBST (µL) | Final conc (µg/mL) |
|---|---|---|---|---|
| A | 2000 | 100 | 100 | 1000 |
| B | 1000 | 100 | 100 | 500 |
| C | 500 | 100 | 100 | 250 |
| D | 250 | 100 | 100 | 125 |
| E | 125 | 100 | 100 | 62.5 |
| F | 62.5 | 100 | 100 | 31.25 |
| G | 31.25 | 100 | 100 | 15.625 |
| H | 15.625 | 100 | 100 | 7.8125 |
| I | 7.8125 | 100 | 100 | 3.90625 |
| J | 0 | 0 | 100 | 0 |

*Sup Table 3: Table illustrating the calculations for the calibration curve used for the Micro BCA analysis.The table also illustrates the measured absorbance values for each standard.*

| Vial | Stock conc (µg/mL) | Vol stock(µL) | Vol PBST (µL) | Final conc (µg/mL) | Abs562 (1) | Abs562 (2) | Abs562 (3) |
|---|---|---|---|---|---|---|---|
| A | 2000 | 100 | 100 | 1000 | 0.518 | 0.406 | 0.471 |
| B | 1000 | 100 | 100 | 500 | 0.411 | 0.419 | 0.432 |
| C | 500 | 100 | 100 | 250 | 0.277 | 0.289 | 0.287 |
| D | 250 | 100 | 100 | 125 | 0.179 | 0.177 | 0.177 |
| E | 125 | 100 | 100 | 62.5 | 0.106 | 0.111 | 0.107 |
| F | 62.5 | 100 | 100 | 31.3 | 0.063 | 0.066 | 0.064 |
| G | 31.3 | 100 | 100 | 15.6 | 0.040 | 0.040 | 0.055 |
| H | 15.6 | 100 | 100 | 7.8 | 0.024 | 0.026 | 0.026 |
| I | 7.8 | 100 | 100 | 3.9 | 0.020 | 0.021 | 0.02 |
| J | 0 | 0 | 100 | 0 | 0.011 | 0.012 | 0.014 |

*Sup Table 4: Measured absorbance values for conjugated antibodies and calculated concentrations obtained from the 4PL model.*

| | Abs562 (1) | Abs562 (2) | Abs562 (3) | OD Mean | Conc (µg/mL) | Adj. Conc (µg/mL) | Volume (µL) | Volume (mL) | Yield (µg) | Conc (mg/mL) |
|---|---|---|---|---|---|---|---|---|---|---|
| 3D6 5:5 | 0.183 | 0.163 | 0.184 | 0.177 | 119.74 | 239.5 | 70 | 0.07 | 16.7636 | 0.24 |
| 3D6 20:5 | 0.207 | 0.002 | 0.200 | 0.202 | 142.45 | 284.9 | 70 | 0.07 | 19.943 | 0.28 |
| RmAb158 5:5 | 0.183 | 0.185 | 0.244 | 0.204 | 144.00 | 288.0 | 73 | 0.073 | 21.024 | 0.29 |
| RmAb158 20:5 | 0.201 | 0.200 | 0.24 | 0.213 | 153.19 | 306.4 | 70 | 0.07 | 21.4466 | 0.31 |

### A.0.2 Biotinylation of Antibodies

*Sup Table 5: Characteristic values for each antibody used in the biotinylation calculations seen in Sup Table 6*

| Antibody | Mw (Da) | Ext. Coeff ($M^{-1}cm^{-1}$) | Ext. coeff (mL*$mg^{-1}cm^{-1}$) |
|---|---|---|---|
| 3D6 | 147400 | 222605 | 1.51 |
| RmAb158 | 148500 | 217565 | 1.46 |

*Sup Table 6: Absorbance values obtained before and after the biotinylation of antibodies 3D6 and RmAb158. This also includes calculations of final concentrations, protein amount and yield. Adj refers to adjustment of the obtained value to the pathlength of the Biodrop.*

| A280 before biot | A280 adj before | Conc before (µg/ml) | Vol (mL) before biot. | A280 after biot. | A280 adj after | Conc after (µg/mL) | Vol (µL) after biot. | Amnt of protein (µg) before biot | 242424 Amnt of protein (µg) after biot | Yield (%) |
|---|---|---|---|---|---|---|---|---|---|---|
| 0.071 | 1.42 | 940 | 0.046 | 0.044 | 0.88 | 628 | 0.07 | 43.25 | 44.00 | 101.7 |
| 0.087 | 1.74 | 1187 | 0.046 | 0.052 | 1.04 | 743 | 0.065 | 54.63 | 48.29 | 88.4 |

*Sup Table 7: Absorbance values with corresponding antibody concentration obtained from the direct ELISA performed to confirm successful biotinylation of 3D6 and RmAb158. Values labeled as "OVER" indicate samples with color development exceeding the measurable absorbance range.*

| Ab conc (nM) | Ab conc (µg/mL) | RmAb Biotin | 3D6 Biotin | Control 3D6 Biotin | Control Biotin Ab |
|---|---|---|---|---|---|
| 10 | 6.4 | OVER | OVER | 3.94325 | OVER |
| 1 | 0.64 | 3.88645 | 3.8645 | 0.4785 | OVER |
| 0.1 | 0.064 | 0.60985 | 0.5634 | 0.09275 | 0.9171 |
| 0.01 | 0.0064 | 0.09985 | 0.0924 | 0.0564 | 0.1357 |
| Blank | 0 | 0.0501 | 0.0494 | 0.05325 | 0.0547 |

### A.0.3 Initial Estimation of Assay Precision

*Sup Table 8: 4PL parameters for each calibration curve during the initial evaluation of assay precision.*

| | | A | B | C | D |
|---|---|---|---|---|---|
| BOLD | Run 1 | 0.125 | 1.287 | 434 | 4.761 |
| | Run 2 | 0.099 | 1.012 | 1240 | 6.237 |
| | Run 3 | 0.100 | 0.972 | 1805 | 6.831 |
| STD | Run 1 | 0.056 | 1.081 | 1114241 | 565.166 |
| | Run 2 | 0.055 | 1.157 | 2353 | 0.871 |
| | Run 3 | 0.054 | 1.119 | 250501 | 64.672 |

# B Supplementary Figures

| Wells | 1 | 2 | 3 | 4 | 5 | 6 | 7 | 8 | 9 | 10 | 11 | 12 |
|---|---|---|---|---|---|---|---|---|---|---|---|---|
| A | 1000 | 1000 | 1000 | 1000 | 1000 | 1000 | 1000 | 1000 | | | | |
| B | 111 | 111 | 111.1 | 111.1 | 111.1 | 111.1 | 111.1 | 111.1 | | | | |
| C | 37.04 | 37.04 | 37.04 | 37.04 | 37.04 | 37.04 | 37.04 | 37.04 | | | | |
| D | 12.35 | 12.35 | 12.35 | 12.35 | 12.35 | 12.35 | 12.35 | 12.35 | | | | |
| E | 4.12 | 4.12 | 4.12 | 4.12 | 4.12 | 4.12 | 4.12 | 4.12 | | | | |
| F | Blank | Blank | Blank | Blank | Blank | Blank | Blank | Blank | | | | |
| G | Blank | Blank | Blank | Blank | Blank | Blank | Blank | Blank | | | | |
| H | 333.3 | 333.3 | 333.3 | 333.3 | 333.3 | 333.3 | 333.3 | 333.3 | | | | |
| | **RmAb158 0.5 µg/mL (5:5)** | | **RmAb158 0.5 µg/mL (20:5)** | | **3D6 0.5 µg/mL (5:5)** | | **3D6 0.5 µg/mL (20:5)** | | | | | |

*Sup Figure 1: Plate layout from evaluating the different Odt-detector antibodies. All concentrations for the antigen displayed in the table are in nM.*

| Wells | 1 | 2 | 3 | 4 | 5 | 6 | 7 | 8 | 9 | 10 | 11 | 12 |
|---|---|---|---|---|---|---|---|---|---|---|---|---|
| A | 1000 | 1000 | 1000 | 1000 | 1000 | 1000 | 1000 | 1000 | 1000 | 1000 | 1000 | 1000 |
| B | 111.11 | 111.11 | 111.11 | 111.11 | 111.11 | 111.11 | 111.11 | 111.11 | 111.11 | 111.11 | 111.11 | 111.11 |
| C | 37.04 | 37.04 | 37.04 | 37.04 | 37.04 | 37.04 | 37.04 | 37.04 | 37.04 | 37.04 | 37.04 | 37.04 |
| D | 12.35 | 12.35 | 12.35 | 12.35 | 12.35 | 12.35 | 12.35 | 12.35 | 12.35 | 12.35 | 12.35 | 12.35 |
| E | 4.12 | 4.12 | 4.12 | 4.12 | 4.12 | 4.12 | 4.12 | 4.12 | 4.12 | 4.12 | 4.12 | 4.12 |
| F | Blank | Blank | Blank | Blank | Blank | Blank | Blank | Blank | Blank | Blank | Blank | Blank |
| G | Blank | Blank | Blank | Blank | Blank | Blank | Blank | Blank | Blank | Blank | Blank | Blank |
| H | 333.3 | 333.3 | 333.3 | 333.3 | 333.3 | 333.3 | 333.3 | 333.3 | 333.3 | 333.3 | 333.3 | 333.3 |
| **Capture:** | RmAb158 1 µg/mL | | | | | | RmAb158 1 µg/mL | | | | | |
| | **100 µL overnight 4°C** | | | | | | **100 µL 120 min 37 °C** | | | | | |
| **Antigen:** | Pf42 | | | | | | | | | | | |
| | 100 µL overnight | | | | | | | | | | | |
| **Detector:** | 3D6 0.05 µg/mL (5:5) | | | | | | | | | | | |
| | **100 µL 180 min** | | **100 µL 120 min** | | **100 µL 60 min** | | **100 µL 180 min** | | **100 µL 120 min** | | **100 µL 60 min** | |
| **SA-HRP:** | SA-HRP 1:200 | | | | | | | | | | | |
| | **100 µL 60 min** | | **100 µL 30 min** | | **100 µL 30 min** | | **100 µL 60 min** | | **100 µL 30 min** | | **100 µL 30 min** | |

*Sup Figure 2: Plate layout from evaluating the different capture and detector antibody incubation times. All concentrations for the antigen displayed in the table are in pM.*

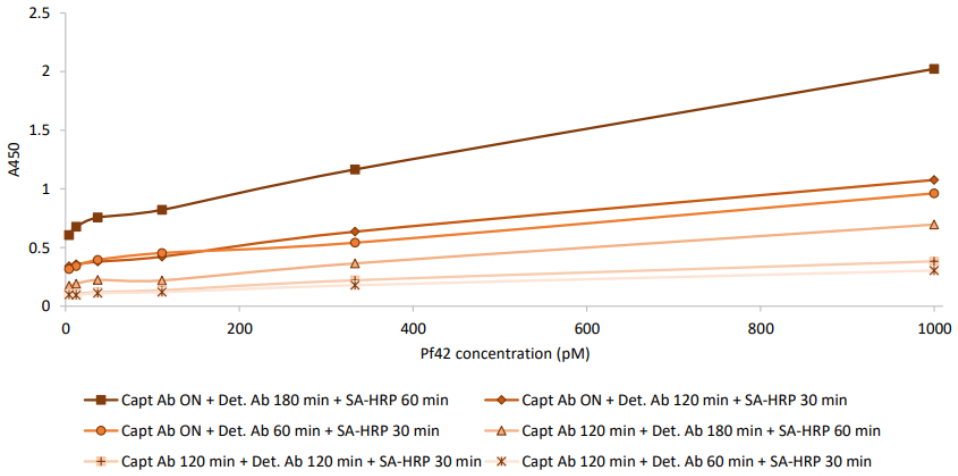


*Sup Figure 3: Mean (n=2) absorbance (450nm) values obtained from the RmAb158 assay in the evaluation of capture and detector antibody incubation time. The highest signal values are only half as strong as those obtained from the 3D6 assay but with the same background noise.*

| Wells | 1 | 2 | 3 | 4 | 5 | 6 | 7 | 8 | 9 | 10 | 11 | 12 |
|---|---|---|---|---|---|---|---|---|---|---|---|---|
| A | 1000 | 1000 | 1000 | 1000 | 1000 | 1000 | | | | | | |
| B | 111.11 | 111.11 | 111.11 | 111.11 | 111.11 | 111.11 | | | | | | |
| C | 37.04 | 37.04 | 37.04 | 37.04 | 37.04 | 37.04 | | | | | | |
| D | 12.35 | 12.35 | 12.35 | 12.35 | 12.35 | 12.35 | | | | | | |
| E | 4.12 | 4.12 | 4.12 | 4.12 | 4.12 | 4.12 | | | | | | |
| F | Blank | Blank | Blank | Blank | Blank | Blank | | | | | | |
| G | Blank | Blank | Blank | Blank | Blank | Blank | | | | | | |
| H | 333.3 | 333.3 | 333.3 | 333.3 | 333.3 | 333.3 | | | | | | |
| **Capture:** | RmAb158 1 µg/mL | | | | | | | | | | | |
| **Blocking:** | 1% Casein | | | | | | | | | | | |
| **Antigen:** | Pf42 | | | | | | | | | | | |
| | **100 µL overnight** | | **100 µL 120 min** | | **100 µL 60 min** | | | | | | | |
| **Detector:** | 3D6 0.05 µg/mL (5:5) | | | | | | | | | | | |
| | 100 µL 60 min | | 100 µL 60 min | | 100 µL 60 min | | | | | | | |

*Sup Figure 4: Plate layout from evaluating the antigen incubation time. All concentrations for the antigen displayed in the table are in pM.*

| **Capture:** | RmAb158 Capture Ab 1 µg/mL in PBS | | | | | | | | | | | | | |
|---|---|---|---|---|---|---|---|---|---|---|---|---|---|---|
| **Blocking:** | 1% Casein in PBS | | | | 2% BSA in PBS | | | | RIA buffer | | | | | |
| Wells | **1** | **2** | **3** | **4** | **5** | **6** | **7** | **8** | **9** | **10** | **11** | **12** | **Detector:** | **Antigen:** |
| A | 12.35 | 4.12 | Blank | Blank | 12.35 | 4.12 | Blank | Blank | 12.35 | 4.12 | Blank | Blank | 3D6 + PBST - 0.5% Casein | Pf42 in PBST + 0.5% Casein |
| B | 12.35 | 4.12 | Blank | Blank | 12.35 | 4.12 | Blank | Blank | 12.35 | 4.12 | Blank | Blank | 3D6 + RIA buffer | |
| C | 12.35 | 4.12 | Blank | Blank | 12.35 | 4.12 | Blank | Blank | 12.35 | 4.12 | Blank | Blank | 3D6 + 1% BSA | |
| D | 12.35 | 4.12 | Blank | Blank | 12.35 | 4.12 | Blank | Blank | 12.35 | 4.12 | Blank | Blank | 3D6 + PBST - 0.5% Casein | Pf42 in PBST + 1% BSA |
| E | 12.35 | 4.12 | Blank | Blank | 12.35 | 4.12 | Blank | Blank | 12.35 | 4.12 | Blank | Blank | 3D6 + RIA buffer | |
| F | 12.35 | 4.12 | Blank | Blank | 12.35 | 4.12 | Blank | Blank | 12.35 | 4.12 | Blank | Blank | 3D6 + 1% BSA | |
| G | | | | | | | | | | | | | | |
| H | | | | | | | | | | | | | | |

*Sup Figure 5: Plate layout from evaluation of blocking buffers and dilution buffers. The plate layout displays the antigen concentration in pM and the different combinations of blocking buffers used in the blocking step, dilution buffers for the antigen and dilution buffers for the OdT-detector antibody. The same diluent was used for the OdT-detector antibody and the SA-HRP.*

| Antigen conc (pM) | Blck Cas + Ag Cas + Det Cas | Blck Cas + Ag Cas + Det RIA | Blck Cas + Ag Cas + Det BSA | Blck BSA + Ag Cas + Det Cas | Blck BSA + Ag Cas + Det RIA | Blck BSA + Ag Cas + Det BSA | Blck RIA + Ag Cas + Det Cas | Blck RIA + Ag Cas + Det RIA | Blck RIA + Ag Cas + Det BSA | Blck Cas + Ag BSA + Det Cas | Blck Cas + Ag BSA + Det RIA | Blck Cas + Ag BSA + Det BSA | Blck BSA + Ag BSA + Det Cas | Blck BSA + Ag BSA + Det RIA | Blck BSA + Ag BSA + Det BSA | Blck RIA + Ag BSA + Det Cas | Blck RIA + Ag BSA + Det RIA | Blck RIA + Ag BSA + Det BSA |
|---|---|---|---|---|---|---|---|---|---|---|---|---|---|---|---|---|---|---|
| 12.37 | 0.1138 | 0.0677 | 0.202 | 0.1337 | 0.0835 | 0.2928 | 0.1315 | 0.085 | 0.3122 | 0.1274 | 0.073 | 0.5812 | 0.1473 | 0.0886 | 0.3504 | 0.1842 | 0.0901 | 0.3662 |
| 4.12 | 0.0888 | 0.0627 | 0.1537 | 0.1198 | 0.0916 | 0.2722 | 0.1053 | 0.0717 | 0.25 | 0.1229 | 0.0635 | 0.1789 | 0.1114 | 0.0819 | 0.2654 | 0.1156 | 0.0744 | 0.2876 |
| 0 | 0.09385 | 0.06095 | 0.16535 | 0.09755 | 0.06945 | 0.26555 | 0.0973 | 0.0638 | 0.20135 | 0.0918 | 0.0603 | 0.15465 | 0.0885 | 0.06565 | 0.2201 | 0.08575 | 0.06105 | 0.2188 |

*Sup Figure 6: Mean OD450 values obtained from the evaluation of blocking agents. The obtained measurements illustrates low background noise When RIA buffer is used as a detector antibody diluent but also low signals overall. Highest background but also signals are given when using 1% BSA as detector antibody diluent.*

| Wells | 1 | 2 | 3 | 4 | 5 | 6 | 7 | 8 | 9 | 10 | 11 | 12 |
|---|---|---|---|---|---|---|---|---|---|---|---|---|
| A | 12.35 | 12.35 | 12.35 | 12.35 | 12.35 | 12.35 | 12.35 | 12.35 | 12.35 | | | |
| B | 4.12 | 4.12 | 4.12 | 4.12 | 4.12 | 4.12 | 4.12 | 4.12 | 4.12 | | | |
| C | 1.37 | 1.37 | 1.37 | 1.37 | 1.37 | 1.37 | 1.37 | 1.37 | 1.37 | | | |
| D | Blank | Blank | Blank | Blank | Blank | Blank | Blank | Blank | Blank | | | |
| E | 12.35 | 12.35 | 12.35 | 12.35 | 12.35 | 12.35 | 12.35 | 12.35 | 12.35 | | | |
| F | 4.12 | 4.12 | 4.12 | 4.12 | 4.12 | 4.12 | 4.12 | 4.12 | 4.12 | | | |
| G | 1.37 | 1.37 | 1.37 | 1.37 | 1.37 | 1.37 | 1.37 | 1.37 | 1.37 | | | |
| H | Blank | Blank | Blank | Blank | Blank | Blank | Blank | Blank | Blank | | | |
| **Capture:** | RmAb158 1 µg/mL | | | | | | | | | | | |
| **Blocking:** | 1% Casein | | | 2% BSA | | | RIA buffer | | | | | |
| **Antigen:** | Pf42 in 1% BSA | | | | | | | | | | | |
| **Detector:** | **3D6 0.05 µg/mL in PBST + 1% BSA** | **3D6 0.1 µg/mL in PBST + 1% BSA** | 3D6 0.2 µg/mL in PBST + 1% BSA | **3D6 0.05 µg/mL in PBST + 0.5% Cas** | **3D6 0.1 µg/mL in PBST + 0.5% Cas** | 3D6 0.2 µg/mL in PBST + 0.5% Cas | **3D6 0.05 µg/mL in PBST + 0.5% Cas** | **3D6 0.1 µg/mL in PBST + 0.5% Cas** | 3D6 0.2 µg/mL in PBST + 0.5% Cas | | | |

*Sup Figure 7: Plate layout from evaluating the different detector antibody concentrations for the final protocol. All concentrations for the antigen displayed in the table are in pM.*

| | BOLD | | | | | | Standard | | | | | |
|---|---|---|---|---|---|---|---|---|---|---|---|---|
| **Wells** | 1 | 2 | 3 | 4 | 5 | 6 | 7 | 8 | 9 | 10 | 11 | 12 |
| A | 1000.00 | 1000.00 | 500.00 | 500.00 | 500.00 | | 1000.00 | 1000.00 | 500.00 | 500.00 | 500.00 | |
| B | 333.33 | 333.33 | 125.00 | 125.00 | 125.00 | | 333.33 | 333.33 | 125.00 | 125.00 | 125.00 | |
| C | 111.11 | 111.11 | 31.25 | 31.25 | 31.25 | | 111.11 | 111.11 | 31.25 | 31.25 | 31.25 | |
| D | 37.04 | 37.04 | 7.81 | 7.81 | 7.81 | | 37.04 | 37.04 | 7.81 | 7.81 | 7.81 | |
| E | 12.35 | 12.35 | Blank | Blank | Blank | | 12.35 | 12.35 | Blank | Blank | Blank | |
| F | 4.12 | 4.12 | Blank | Blank | Blank | | 4.12 | 4.12 | Blank | Blank | Blank | |
| G | Blank | Blank | Blank | Blank | Blank | | Blank | Blank | Blank | Blank | Blank | |
| H | Blank | Blank | Blank | Blank | Blank | | Blank | Blank | Blank | Blank | Blank | |
| **Capture:** | RmAb158 1 µg/mL | | | | | | | | | | | |
| | 100 µL overnight 4°C | | | | | | | | | | | |
| **Blocking:** | 2% BSA | | | | | | | | | | | |
| | 300 µL 120 min | | | | | | | | | | | |
| **Antigen:** | Pf42 in 1% BSA | | | | | | | | | | | |
| | 100 µL overnight | | | | | | | | | | | |
| **Detector:** | 3D6 0.1 µg/mL in PBST + 0.5% Cas | | | | | | | | | | | |
| | 100 µL 60 min | | | | | | | | | | | |
| **SA-HRP:** | SA-HRP 1:200 | | | | | | | | | | | |
| | 100 µL 30 min | | | | | | | | | | | |

*Sup Figure 8: Representative plate layout from the initial evaluation of assay precision. All concentrations for the antigen displayed in the table are in pM.*

| Antigen conc (pM) | Run 1 | | Run 2 | | Run 3 | |
|---|---|---|---|---|---|---|
| | Rep 1 | Rep 2 | Rep 1 | Rep 2 | Rep 1 | Rep 2 |
| 1000 | 3.5895 | 3.5682 | 2.9444 | 2.7259 | 2.5141 | 2.5377 |
| 333.3 | 2.0101 | 2.1023 | 1.3938 | 1.3766 | 1.1851 | 1.1946 |
| 111.1 | 0.8592 | 0.734 | 0.5574 | 0.6148 | 0.531 | 0.5249 |
| 37.04 | 0.3196 | 0.34 | 0.2694 | 0.2888 | 0.2397 | 0.2398 |
| 12.35 | 0.1764 | 0.1749 | 0.1492 | 0.1527 | 0.1617 | 0.1475 |
| 4.12 | 0.1234 | 0.1236 | 0.1195 | 0.1184 | 0.1247 | 0.1178 |
| 0 | 0.1018 | 0.0995 | 0.1045 | 0.1021 | 0.107 | 0.1129 |

*(a) BOLD*

| Antigen conc (pM) | Run 1 | | Run 2 | | Run 3 | |
|---|---|---|---|---|---|---|
| | Rep 1 | Rep 2 | Rep 1 | Rep 2 | Rep 1 | Rep 2 |
| 1000 | 0.3492 | 0.3381 | 0.2797 | 0.2721 | 0.194 | 0.1805 |
| 333.3 | 0.1413 | 0.1432 | 0.1304 | 0.1336 | 0.0947 | 0.0908 |
| 111.1 | 0.0842 | 0.0843 | 0.0778 | 0.0781 | 0.0656 | 0.0658 |
| 37.04 | 0.0626 | 0.0645 | 0.0612 | 0.0625 | 0.0572 | 0.056 |
| 12.35 | 0.056 | 0.0614 | 0.0554 | 0.0591 | 0.0546 | 0.0541 |
| 4.12 | 0.054 | 0.0556 | 0.0553 | 0.0549 | 0.0516 | 0.0577 |
| 0 | 0.0521 | 0.0529 | 0.0546 | 0.0529 | 0.0515 | 0.052 |

*(b) Standard*

*Sup Figure 9: Obtained raw absorbance (450 nm) values for the calibration curves obtained from each run during the initial evaluation of assay precision. Samples were run in duplicates. (a) BOLD-amplified calibration curve (b) Standard calibration curve*

| | Run 1 | | | Run 2 | | | Run 3 | | |
|---|---|---|---|---|---|---|---|---|---|
| Sample | Rep 1 | Rep 2 | Rep 3 | Rep 1 | Rep 2 | Rep 3 | Rep 1 | Rep 2 | Rep 3 |
| 1 | 2.616 | 2.5279 | 2.6185 | 2.6249 | 2.6223 | 2.5709 | 2.5558 | 2.6184 | 2.6261 |
| 2 | 0.9674 | 0.9085 | 0.9104 | 1.0022 | 0.9417 | 0.916 | 0.9844 | 1.0053 | 0.9897 |
| 3 | 0.3366 | 0.3058 | 0.3327 | 0.3185 | 0.3325 | 0.3048 | 0.3363 | 0.373 | 0.3563 |
| 4 | 0.169 | 0.1546 | 0.1563 | 0.1486 | 0.154 | 0.1504 | 0.1606 | 0.1717 | 0.1713 |

*(a) BOLD*

| | Run 1 | | | Run 2 | | | Run 3 | | |
|---|---|---|---|---|---|---|---|---|---|
| Sample | Rep 1 | Rep 2 | Rep 3 | Rep 1 | Rep 2 | Rep 3 | Rep 1 | Rep 2 | Rep 3 |
| 1 | 0.1921 | 0.1908 | 0.2076 | 0.2173 | 0.2224 | 0.2444 | 0.1829 | 0.1789 | 0.1947 |
| 2 | 0.09 | 0.0889 | 0.0939 | 0.0928 | 0.0945 | 0.1022 | 0.0809 | 0.0822 | 0.0867 |
| 3 | 0.0608 | 0.0637 | 0.0642 | 0.064 | 0.0634 | 0.0673 | 0.0581 | 0.0606 | 0.0605 |
| 4 | 0.0535 | 0.0555 | 0.0555 | 0.0583 | 0.0592 | 0.0577 | 0.0535 | 0.0531 | 0.0535 |

*(b) Standard*

*Sup Figure 10: Obtained raw absorbance (450 nm) values for the control samples obtained from each run during the initial evaluation of assay precision. Samples were run in triplicates.(a) Control samples from BOLD-amplified assay (b) Control samples from standard assay*

# C Supplementary Methods

**RIA buffer reagents**

1000 mL dH2O
1% BSA
350 mM NaCl
10 mM Tris-HCl (pH 7.6)
1% Tween 20
1% SDS

*Sup Table 9: Buffers, reagents, and assay workflow for the final BOLD-amplified format, including key incubation steps and detection components.*

| Step | Description | Reagent / buffer | Incubation conditions | Source |
|---|---|---|---|---|
| 1 | Preparation of capture antibody (RmAb158) surface. | PBS, pH 7.4 | 100 µL of 1 µg/mL RmAb158, incubated overnight at 2–8 °C. | Protein design group, UU and Medicago 09-2051-100 |
| | Washing | PBS, pH 7.4 + 0.05% Tween-20® (PBS-T) | 8x400 µL | Medicago 09-9410-100 |
| 2 | Blocking | 2% BSA in PBS, pH 7.4 | 300 µL, incubated 60 min at 20–25 °C. | Sigma-Aldrich A7906 and Medicago 09-2051-100 |
| | Washing | PBS, pH 7.4 + 0.05% Tween-20® (PBS-T) | 3x400 µL | Medicago 09-9410-100 |
| 3 | Preparation of Pf42 calibrators or samples. | PBS, pH 7.4 + 0.05% Tween-20® and 1% BSA | 100 µL of calibrators or sample, incubated overnight at 2–8 °C. | Medicago 09-9410-100, Sigma-Aldrich A7906 and Protein design group, UU |
| | Washing | PBS-T | 8x400 µL | Medicago 09-9410-100 |
| 4 | Binding of conjugated detector antibody (3D6 5:5) to Pf42 calibrators and samples. | PBS, pH 7.4 + 0.05% Tween-20® and 0.5% Casein (PBS-TC) | 100 µL of 0.1 µg/mL detector antibody, incubated 60 min at 20–25 °C. | Medicago 09-9410-100, Thermofisher Scientific 37528 |
| | Washing | PBS-T | 8x400 µL | - |
| 5 | BOLD polymerization, generation of DNA/RNA hybrid strand. | Exazym® Polymerase Reaction kit | 100 µl: 23 µL Reaction Solution (with Template) + 77 µL Polymerase Working Solution, incubated 30 min at 20–25 °C. | Cavidi 10-1001-01 |
| | Washing | PBS-T | 8x400 µL | - |
| 6 | BOLD detection – binding of biotinylated anti-BrdU antibodies to DNA/RNA hybrid strand. | Exazym® Biotin Detection kit. | 100 µL Antibody Biotin Working Solution, incubated 30 min at 20–25 °C. | Cavidi 10-2001-01 |
| | Washing | PBS-T | 8x400 µL | - |
| 7 | Binding of streptavidin conjugate to biotinylated anti-BrdU antibodies. | SA-HRP. Dilution with PBS-TC | 100 µL of SA-HRP, incubated 30 min at 20–25 °C. | R&D Systems DY998 |
| | Washing | PBS-T | 8x400 µL | - |
| 8 | Colorimetric detection – TMB development, stopped with 2 M $H_2SO_4$; absorbance read at 450 nm. | 1-Step™ TMB ELISA substrate and stop solution 2M $H_2SO_4$. | 100 µL of TMB substrate, incubated 30 min at 20–25 °C. | Thermo Fisher Scientific 34028 and Merck 1.60315.1000 |

*Sup Table 10: Buffers, reagents, and assay workflow for the standard format, including key incubation steps and detection components.*

| Step | Description | Reagent / buffer | Incubation conditions | Source |
|---|---|---|---|---|
| 1 | Preparation of capture antibody (RmAb158) surface. | PBS, pH 7.4 | 100 µL of 1 µg/mL RmAb158, incubated overnight at 2–8 °C. | Protein design group, UU and Medicago 09-2051-100 |
| | Washing | PBS, pH 7.4 + 0.05% Tween-20® (PBS-T) | 3x400 µL | Medicago 09-9410-100 |
| 2 | Blocking | 2% BSA in PBS, pH 7.4 | 300 µL, incubated 60 min at 20–25 °C. | Sigma-Aldrich A7906 and Medicago 09-2051-100 |
| | Washing | PBS, pH 7.4 + 0.05% Tween-20® (PBS-T) | 3x400 µL | Medicago 09-9410-100 |
| 3 | Preparation of Pf42 calibrators or samples. | PBS, pH 7.4 + 0.05% Tween-20® and 1% BSA | 100 µL of calibrators or sample, incubated overnight at 2–8 °C. | Medicago 09-9410-100, Sigma-Aldrich A7906 and Protein design group, UU |
| | Washing | PBS-T | 3x400 µL | Medicago 09-9410-100 |
| 4 | Binding of biotinylated detector antibody (3D6) to Pf42 calibrators and samples. | PBS, pH 7.4 + 0.05% Tween-20® and 0.5% Casein (PBS-TC) | 100 µL of 1 µg/mL detector antibody, incubated 60 min at 20–25 °C. | Medicago 09-9410-100, Thermofisher Scientific 37528 |
| | Washing | PBS-T | 3x400 µL | - |
| 5 | Binding of streptavidin conjugate to biotinylated anti-BrdU antibodies. | SA-HRP. Dilution with PBS-TC | 100 µL of SA-HRP, incubated 30 min at 20–25 °C. | R&D Systems DY998 |
| | Washing | PBS-T | 3x400 µL | - |
| 6 | Colorimetric detection – TMB development, stopped with 2 M $H_2SO_4$; absorbance read at 450 nm. | 1-Step™ TMB ELISA substrate and stop solution 2M $H_2SO_4$. | 100 µL of TMB substrate, incubated 30 min at 20–25 °C. | Thermo Fisher Scientific 34028 and Merck 1.60315.1000 |

# D Code Details

## D.1 Code Used in the BCA Analysis:

```
# ========================
# BCA analysis (4PL)
# ========================

import numpy as np
import pandas as pd
import matplotlib.pyplot as plt
from scipy.optimize import curve_fit

# 1. Load Excel
df = pd.read_excel(r"C:/Users/serne/Downloads/BCA_ELISA_scipts/BCA.xlsx")

# First row contains headers → fix dataframe
df.columns = df.iloc[0]
df = df.iloc[1:].reset_index(drop=True)

# Clean column names
df.columns = (
    df.columns
    .astype(str)
    .str.strip()
    .str.replace("\n", " ")
)

print(df.columns)
print(df.shape)

# Select standards only
standards = df[df["Vial"].isin(list("ABCDEFGHIJ"))].copy()

# Concentrations (use FINAL concentration for BCA)
x = pd.to_numeric(
    standards["Final conc (µg/mL)"], errors="coerce"
)

# OD replicates
y_reps = standards[["Abs562 (1)", "Abs562 (2)", "Abs562 (3)"]].apply(
    pd.to_numeric, errors="coerce"
)

# Mean + SD
y_mean = y_reps.mean(axis=1)
y_sd   = y_reps.std(axis=1, ddof=1)

# Remove invalid points
mask = (~x.isna()) & (~y_mean.isna()) & (x > 0)

x_fit = x[mask].to_numpy()
y_fit = y_mean[mask].to_numpy()
y_sd_fit = y_sd[mask].to_numpy()

# 4PL model
def log4pl(x, A, B, C, D):
    return (A - D) / (1 + (x / C)**B) + D
```

```
55
56 # Initial guesses
57 p0 = [min(y_fit), 1.0, np.median(x_fit), max(y_fit)]
58
59 params, _ = curve_fit(
60     log4pl,
61     x_fit,
62     y_fit,
63     p0=p0,
64     maxfev=10000
65 )
66
67 A, B, C, D = params
68
69 print(
70     f"4PL parameters:\n"
71     f"A = {A:.4f}, B = {B:.4f}, C = {C:.4f}, D = {D:.4f}"
72 )
73
74 # Plot standard curve
75 x_plot = np.logspace(np.log10(min(x_fit)), np.log10(max(x_fit)), 500)
76 y_plot = log4pl(x_plot, A, B, C, D)
77
78 plt.errorbar(
79     x_fit, y_fit, yerr=y_sd_fit,
80     fmt='o', capsize=4, label="Standards (mean ± SD)"
81 )
82 plt.plot(x_plot, y_plot, label="4PL fit")
83
84 plt.xscale("log")
85 plt.xlabel("Concentration (µg/mL)")
86 plt.ylabel("OD562")
87 plt.legend()
88 plt.grid(True)
89 plt.tight_layout()
90 plt.show()
91
92
93 # Invert 4PL (OD → conc)
94 def invert_4pl(y, A, B, C, D):
95     if y <= A or y >= D:
96         return np.nan
97     return C * (((A - D) / (y - D) - 1) ** (1 / B))
98
99
100 # Interpolate unknown samples
101 samples = df[~df["Vial"].isin(list("ABCDEFGHIJ"))].copy()
102
103 sample_reps = samples[["Abs562 (1)", "Abs562 (2)", "Abs562 (3)"]].apply(
104     pd.to_numeric, errors="coerce"
105 )
106
107 samples["OD mean"] = sample_reps.mean(axis=1)
108 samples["OD SD"]   = sample_reps.std(axis=1, ddof=1)
109
110 # Example dilution factor (change if needed)
111 DILUTION_FACTOR = 2
112
113 samples["Conc (µg/mL) diluted"] = samples["OD mean"].apply(
114     lambda y: invert_4pl(y, A, B, C, D)
115 )
116
```

```
samples["Conc (µg/mL) original"] = (
    samples["Conc (µg/mL) diluted"] * DILUTION_FACTOR
)

print("\nSample results:")
print(
    samples[
        ["Vial", "OD mean", "OD SD",
         "Conc (µg/mL) diluted", "Conc (µg/mL) original"]
    ]
)

#Assess how well the model fits to the expected standard curve (corresponding to R2 values)
y_pred = log4pl(x_fit, A, B, C, D)
recovery = (y_pred / y_fit) * 100
print(f"{'Conc (µg/mL)':>12} {'OD mean':>10} {'Predicted OD':>15} {'Recovery (%)':>15}")
for conc, od, pred, rec in zip(x_fit, y_fit, y_pred, recovery):
    print(f"{conc:12.3f} {od:10.3f} {pred:15.3f} {rec:15.2f}")
```

## D.2 Code Used in the ELISA Precision Analysis :

```
# ==========================
# ELISA analysis (4PL) - BOLD and Standard fitted separately
# ==========================

import numpy as np
import pandas as pd
import matplotlib.pyplot as plt
from scipy.optimize import curve_fit

# ==========================
# 1. Load and split datasets
# ==========================

df_raw = pd.read_excel("/mnt/user-data/uploads/ELISA_4PL_data.xlsx", header=None)

# Find rows where the header row repeats (i.e. "Row" appears in column 0)
header_rows = df_raw.index[df_raw.iloc[:, 0] == "Row"].tolist()

datasets = {}
labels = ["BOLD", "Standard"]

for i, label in enumerate(labels):
    start = header_rows[i]
    end = header_rows[i + 1] if i + 1 < len(header_rows) else len(df_raw)

    block = df_raw.iloc[start:end].copy()
    block.columns = block.iloc[0].astype(str).str.strip().str.replace("\n", " ")
    block = block.iloc[1:].reset_index(drop=True)
    block.columns = block.columns.str.strip()
    block["Sample"] = block["Sample "].astype(str).str.strip() if "Sample " in block.columns else block["Sample"].astype(str).str.strip()

    datasets[label] = block

# ==========================
# 4PL model and inversion
```

```
# ==========================

def log4pl(x, A, B, C, D):
    return (A - D) / (1 + (x / C) ** B) + D

def invert_4pl(y, A, B, C, D):
    if y <= min(A, D) or y >= max(A, D):
        return np.nan
    return C * (((A - D) / (y - D) - 1) ** (1 / B))

# ==========================
# 2. Fit curve + compute LOD/LLOQ per dataset
# ==========================

results = {}
fig, axes = plt.subplots(1, 2, figsize=(14, 6))

for ax, (label, df) in zip(axes, datasets.items()):

    # --- Standards ---
    standards = df[df["Row"].isin(list("ABCDEFG"))].copy()
    x = pd.to_numeric(standards["Antigen conc (pM)"], errors="coerce")
    y_reps = standards[["Std curve 1", "Std curve 2"]].apply(pd.to_numeric, errors="
    coerce")
    y_mean = y_reps.mean(axis=1)
    y_sd = y_reps.std(axis=1, ddof=1)

    mask = (~x.isna()) & (~y_mean.isna()) & (x > 0)
    x_fit = x[mask].to_numpy()
    y_fit = y_mean[mask].to_numpy()
    y_sd_fit = y_sd[mask].to_numpy()

    p0 = [min(y_fit), 1.0, np.median(x_fit), max(y_fit)]
    params, _ = curve_fit(log4pl, x_fit, y_fit, p0=p0, maxfev=10000)
    A, B, C, D = params

    print(f"\n{'='*40}")
    print(f"{label} - 4PL parameters:")
    print(f"  A (min asymptote) = {A:.4f}")
    print(f"  B (Hill slope)    = {B:.4f}")
    print(f"  C (EC50)          = {C:.4f}")
    print(f"  D (max asymptote) = {D:.4f}")

    # --- Blank row ---
    blank_row = df[df["Row"] == "G"].copy()
    blank_vals = pd.to_numeric(
        blank_row[["Std curve 1", "Std curve 2"]].values.flatten(),
        errors="coerce"
    )
    blank_vals = blank_vals[~np.isnan(blank_vals)]
    blank_mean = blank_vals.mean()
    blank_sd = blank_vals.std(ddof=1)

    lod_od   = blank_mean + 3  * blank_sd
    lloq_od  = blank_mean + 10 * blank_sd

    lod_conc  = invert_4pl(lod_od,  A, B, C, D)
    lloq_conc = invert_4pl(lloq_od, A, B, C, D)

    print(f"\n{label} - Blank statistics:")
    print(f"  n            = {len(blank_vals)}")
    print(f"  Mean OD      = {blank_mean:.4f}")
```

```
    print(f"  SD           = {blank_sd:.4f}")
    print(f"\n{label} - Detection limits:")
    print(f"  LOD  (OD)    = {lod_od:.4f}  → {lod_conc:.3f} pM" if not np.isnan(lod_conc)  else f"  LOD  (OD)    = {lod_od:.4f}  → outside curve range")
    print(f"  LLOQ (OD)    = {lloq_od:.4f}  → {lloq_conc:.3f} pM" if not np.isnan(lloq_conc) else f"  LLOQ (OD)    = {lloq_od:.4f}  → outside curve range")

    # --- Samples ---
    samples = df[df["Sample"].isin(["1", "2", "3", "4"])].copy()
    sample_reps = samples[["Rep 1 ", "Rep 2 ", "Rep 3 "]].apply(pd.to_numeric, errors="coerce")
    samples = samples.copy()
    samples["OD mean"] = sample_reps.mean(axis=1)
    samples["OD SD"]   = sample_reps.std(axis=1, ddof=1)
    samples["%CV"]     = (samples["OD SD"] / samples["OD mean"]) * 100
    samples["Conc (pM)"] = samples["OD mean"].apply(lambda y: invert_4pl(y, A, B, C, D))

    print(f"\n{label} - Sample results:")
    print(samples[["Row", "Sample", "OD mean", "OD SD", "%CV", "Conc (pM)"]].to_string(index=False))

    results[label] = {
        "params": (A, B, C, D),
        "blank_mean": blank_mean,
        "blank_sd": blank_sd,
        "lod_od": lod_od,
        "lloq_od": lloq_od,
        "lod_conc": lod_conc,
        "lloq_conc": lloq_conc,
        "samples": samples,
        "x_fit": x_fit,
        "y_fit": y_fit,
        "y_sd_fit": y_sd_fit,
    }

    # --- Plot ---
    x_plot = np.logspace(np.log10(min(x_fit)), np.log10(max(x_fit)), 500)
    y_plot = log4pl(x_plot, A, B, C, D)

    ax.errorbar(x_fit, y_fit, yerr=y_sd_fit, fmt='o', capsize=4, label="Standards (mean ± SD)")
    ax.plot(x_plot, y_plot, label="4PL fit")

    valid_samples = samples.dropna(subset=["Conc (pM)", "OD mean"])
    ax.errorbar(
        valid_samples["Conc (pM)"], valid_samples["OD mean"],
        yerr=valid_samples["OD SD"], fmt='s', markersize=7,
        capsize=4, label="Samples"
    )

    # LOD / LLOQ lines
    if not np.isnan(lod_conc):
        ax.axvline(lod_conc,  color="orange", linestyle="--", linewidth=1, label=f"LOD {lod_conc:.2f} pM")
    if not np.isnan(lloq_conc):
        ax.axvline(lloq_conc, color="red",    linestyle="--", linewidth=1, label=f"LLOQ {lloq_conc:.2f} pM")

    ax.set_xscale("log")
    ax.set_xlabel("Concentration (pM)")
    ax.set_ylabel("OD450")
```

```
    ax.set_title(label)
    ax.legend(fontsize=8)
    ax.grid(True)

plt.tight_layout()
plt.savefig("/mnt/user-data/outputs/ELISA_4PL_dual.png", dpi=150)
plt.show()
print("\nPlot saved to ELISA_4PL_dual.png")

# ========================
# 3. Export results to Excel
# ========================

output_path = "/mnt/user-data/outputs/ELISA_dual_results.xlsx"
with pd.ExcelWriter(output_path, engine="openpyxl") as writer:
    for label, res in results.items():
        A, B, C, D = res["params"]
        summary = pd.DataFrame({
            "Parameter": ["A (min asymptote)", "B (Hill slope)", "C (EC50)", "D (max asymptote)",
                          "Blank mean (OD)", "Blank SD (OD)",
                          "LOD (OD)", "LOD (pM)", "LLOQ (OD)", "LLOQ (pM)"],
            "Value": [round(A, 4), round(B, 4), round(C, 4), round(D, 4),
                      round(res["blank_mean"], 4), round(res["blank_sd"], 4),
                      round(res["lod_od"], 4),
                      round(res["lod_conc"], 3) if not np.isnan(res["lod_conc"]) else "outside range",
                      round(res["lloq_od"], 4),
                      round(res["lloq_conc"], 3) if not np.isnan(res["lloq_conc"]) else "outside range"]
        })
        summary.to_excel(writer, sheet_name=f"{label}_summary", index=False)

        export_df = res["samples"][["Row", "Sample", "OD mean", "OD SD", "%CV", "Conc (pM)"]].copy()
        export_df = export_df.round({"OD mean": 3, "OD SD": 3, "%CV": 2, "Conc (pM)": 3})
        export_df.to_excel(writer, sheet_name=f"{label}_samples", index=False)

print(f"Results exported to: {output_path}")
```